

## RESEARCH ARTICLE

# Ammonia exposure affects the mRNA and protein expression levels of certain Rhesus glycoproteins in the gills of climbing perch

Xiu L. Chen<sup>1</sup>, Biyan Zhang<sup>1</sup>, You R. Chng<sup>1</sup>, Jasmine L. Y. Ong<sup>1</sup>, Shit F. Chew<sup>2</sup>, Wai P. Wong<sup>1</sup>, Siew H. Lam<sup>1,3</sup>, Tsutomu Nakada<sup>4</sup> and Yuen K. Ip<sup>1,\*</sup>

## ABSTRACT

The freshwater climbing perch, *Anabas testudineus*, is an obligate air-breathing and euryhaline teleost capable of active ammonia excretion and tolerant of high concentrations of environmental ammonia. As Rhesus glycoproteins (RhGP/Rhgp) are known to transport ammonia, this study aimed to obtain the complete cDNA coding sequences of various *rhgp* isoforms from the gills of *A. testudineus*, and to determine their mRNA and protein expression levels during 6 days of exposure to 100 mmol l<sup>-1</sup> NH<sub>4</sub>Cl. The subcellular localization of Rhgp isoforms in the branchial epithelium was also examined in order to elucidate the type of ionocyte involved in active ammonia excretion. Four *rhgp* (*rhag*, *rhbg*, *rhcg1* and *rhcg2*) had been identified from the gills of *A. testudineus*. They had conserved amino acid residues for NH<sub>4</sub><sup>+</sup> binding, NH<sub>4</sub><sup>+</sup> deprotonation, channel gating and lining of the vestibules. Despite inwardly directed NH<sub>3</sub> and NH<sub>4</sub><sup>+</sup> gradients, there were significant increases in the mRNA expression levels of the four branchial *rhgp* in *A. testudineus* at certain time points during 6 days of ammonia exposure, with significant increases in the protein abundances of Rhag and Rhcg2 on day 6. Immunofluorescence microscopy revealed a type of ammonia-inducible Na<sup>+</sup>/K<sup>+</sup>-ATPase  $\alpha$ 1c-immunoreactive ionocyte with apical Rhag and basolateral Rhcg2 in the gills of fish exposed to ammonia for 6 days. Hence, active ammonia excretion may involve NH<sub>4</sub><sup>+</sup> entering the ionocyte through the basolateral Rhcg2 and being excreted through the apical Rhag, driven by a transapical membrane electrical potential generated by the apical cystic fibrosis transmembrane conductance regulator Cl<sup>-</sup> channel, as suggested previously.

**KEY WORDS:** Air-breathing fish, Active ammonia excretion, Ammonia transporters, Ionocyte, Nitrogen metabolism

## INTRODUCTION

The climbing perch, *Anabas testudineus* (Bloch 1792), is a freshwater teleost belonging to Order Perciformes and Family Anabantidae. It can be found in canals, lakes, ponds, swamps and estuaries in tropical Asia, and can tolerate extremely unfavorable water conditions (Pethiyagoda, 1991). It has special accessory

breathing organs in the upper part of its gill chambers to facilitate the utilization of atmospheric air (Hughes and Munshi, 1973; Munshi et al., 1986; Graham, 1997). Occasionally, it gulps air from the water surface, and the air is channelled to the accessory breathing organs for gaseous exchange. *Anabas testudineus* is ammonotelic, excreting ammonia as the predominant nitrogenous waste. It cannot detoxify ammonia to urea as it does not possess a functional hepatic ornithine-urea cycle in its liver (Tay et al., 2006). Although many teleosts succumb to 1–5 mmol l<sup>-1</sup> of ammonia within several hours, *A. testudineus* can actively excrete ammonia against large inwardly directed P<sub>NH<sub>3</sub></sub> and NH<sub>4</sub><sup>+</sup> gradients and survive in water containing 100 mmol l<sup>-1</sup> of NH<sub>4</sub>Cl for many days (Loong et al., 2011; Ip et al., 2012a,b).

Recently, it has been reported that active NH<sub>4</sub><sup>+</sup> excretion in freshwater containing high concentrations of ammonia and active Na<sup>+</sup> excretion in seawater through the gills of *A. testudineus* may involve similar transport mechanisms, including Na<sup>+</sup>/K<sup>+</sup>-ATPase (Nka) (Ip et al., 2012a), Na<sup>+</sup>:K<sup>+</sup>:2Cl<sup>-</sup> cotransporter 1a (Nkcc1a) (Loong et al., 2011), and cystic fibrosis transmembrane conductance regulator Cl<sup>-</sup> channel (Cfr) (Ip et al., 2012b). Basolateral Nkcc1a can transport NH<sub>4</sub><sup>+</sup>, in substitution for K<sup>+</sup> and together with Na<sup>+</sup> and Cl<sup>-</sup>, into ionocytes, down the electrochemical gradient of Na<sup>+</sup> (Loong et al., 2011), while basolateral Nka actively transports Na<sup>+</sup> out of and K<sup>+</sup> into the cell to maintain intracellular Na<sup>+</sup> and K<sup>+</sup> homeostasis (Ip et al., 2012a). Active NH<sub>4</sub><sup>+</sup> excretion across the apical membrane of ionocytes in the gills of *A. testudineus* could be driven by an electrical potential generated by anion (HCO<sub>3</sub><sup>-</sup>/Cl<sup>-</sup>) excretion through the apical Cfr (Ip et al., 2012b). However, how NH<sub>4</sub><sup>+</sup> exits the apical membrane of ionocytes in the gills of *A. testudineus* is an enigma.

Rhesus family glycoproteins (RhGP) belong to a superfamily of ammonium transporters (AMT), which includes methylammonium permeases (MEP) (Huang and Peng, 2005; Nakhoul and Hamm, 2014). They consist of the erythroid Rh-associated glycoprotein (RhAG) and two non-erythroid members: Rh family B glycoprotein (RhBG) and Rh family C glycoprotein (RhCG) (Nakhoul and Hamm, 2013, 2014). Genes encoding ammonia transporters were first identified from the plant *Arabidopsis thaliana* (*AtAmt*) and yeast *Saccharomyces cerevisiae* (*ScMep1*) (Ninnemann et al., 1994; Marini et al., 1994). Initial studies on yeast mutants provided the first evidence on the possible involvement of Rhgp in NH<sub>4</sub><sup>+</sup> transport (Marini et al., 2000), and the possible role of Rhgp in NH<sub>4</sub><sup>+</sup> transport in fish was first demonstrated in the gills of the pufferfish *Takifugu rubripes* (Nakada et al., 2007a). After identifying *rhag*, *rhbg*, *rhcg1* and *rhcg2*, Nakada et al. (2007a) expressed them in *Xenopus* oocytes and showed that the encoded proteins facilitated uptake of methylammonium (CH<sub>3</sub>NH<sub>3</sub><sup>+</sup>), which is an analogue of NH<sub>4</sub><sup>+</sup>. Basal levels of plasma ammonia in *T. rubripes* are maintained by the passive movement of ammonia across the pavement cells

<sup>1</sup>Department of Biological Sciences, National University of Singapore, Kent Ridge, Singapore 117543, Republic of Singapore. <sup>2</sup>Natural Sciences and Science Education, National Institute of Education, Nanyang Technological University, 1 Nanyang Walk, Singapore 637616, Republic of Singapore. <sup>3</sup>NUS Environmental Research Institute, National University of Singapore, Kent Ridge, Singapore 117411, Republic of Singapore. <sup>4</sup>Department of Molecular Pharmacology, Shinshu University School of Medicine, Matsumoto, Nagano 390-8621, Japan.

\*Author for correspondence (dbsipyk@nus.edu.sg)

 Y.K.I., 0000-0001-9124-7911

**List of symbols and abbreviations**

AMT	ammonium transporter
Cftr/CFTR	cystic fibrosis transmembrane conductance regulator Cl <sup>-</sup> channel
MEP	methylammonium permease
Nka/NKA	Na <sup>+</sup> /K <sup>+</sup> -ATPase
Nka $\alpha$ 1c	Na <sup>+</sup> /K <sup>+</sup> -ATPase $\alpha$ 1c
Nkcc1/NKCC1	Na <sup>+</sup> :K <sup>+</sup> :2Cl <sup>-</sup> cotransporter 1
Nkcc1a	Na <sup>+</sup> :K <sup>+</sup> :2Cl <sup>-</sup> cotransporter 1a
Rhag/RhAG	Rh blood group-associated glycoprotein
Rhbg/RhBG	Rh family B glycoprotein
Rhcg/RhCG	Rh family C glycoprotein
Rhcg1	Rhesus family C glycoprotein 1
Rhcg2	Rhesus family C glycoprotein 2
Rhgp/RhGP	Rhesus glycoproteins

through basolateral Rhbg and apical Rhcg2 (Nawata et al., 2010). However, upon exposure of *T. rubripes* to 1 or 5 mmol l<sup>-1</sup> NH<sub>4</sub>HCO<sub>3</sub>, active ammonia excretion occurs through some kind of ionocytes with the involvement of Nka and Rhcg1 (Nawata et al., 2010).

Although these studies collectively support the functional role of RhGP/Rhgp in ammonia transport, whether they transport NH<sub>3</sub> or NH<sub>4</sub><sup>+</sup> and whether they act as a channel or a transporter remain controversial. In fact, a previous study provided evidence to suggest RhGP as NH<sub>3</sub> channels (Ripoche et al., 2004), whereas others suggested them to be electrogenic NH<sub>4</sub><sup>+</sup> transporters (Nakhoul et al., 2006; Nakada et al., 2007a) or dual transporters of NH<sub>3</sub> and NH<sub>4</sub><sup>+</sup> (Bakouh et al., 2004; Benjelloun et al., 2005). However, with primary reference to the X-ray crystallographic structure of AmtB of *Escherichia coli* (EcAmtB; Khademi et al., 2004), the majority of reports on fish Rhgp regard them as NH<sub>3</sub> channels (see Wright and Wood, 2009; Weihrauch et al., 2009; Hwang et al., 2011 for reviews). EcAmtB is a homolog of RhGP, but in *E. coli*, it is involved in ammonia uptake instead of ammonia excretion (Khademi et al., 2004; Khademi and Stroud, 2006). Members of the AMT/MEP/RhGP family are trimeric proteins, with each monomer consisting of a 20 Å hydrophobic channel. The first binding site facing the extracellular medium serves as a vestibule that recruits NH<sub>3</sub> or NH<sub>4</sub><sup>+</sup>, with preference for NH<sub>4</sub><sup>+</sup>. The recruited NH<sub>4</sub><sup>+</sup> is deprotonated and the H<sup>+</sup> is released extracellularly while NH<sub>3</sub> is conducted through the hydrophobic pore. On the intracellular side, NH<sub>3</sub> recruits an intracellular H<sup>+</sup> and is released as NH<sub>4</sub><sup>+</sup>.

Because there is indirect evidence that suggests NH<sub>4</sub><sup>+</sup> as the species of ammonia being actively excreted by *A. testudineus* during environmental ammonia exposure (Tay et al., 2006; Loong et al., 2011; Ip et al., 2012a,b), the present study was undertaken to obtain the complete sequences of *rhag*, *rhbg*, *rhcg1* and *rhcg2* from the gills of *A. testudineus* and to perform molecular characterization on their deduced amino acid sequences. Furthermore, efforts were made to examine, using quantitative real-time PCR (qPCR), the effects of environmental ammonia exposure (100 mmol l<sup>-1</sup> of NH<sub>4</sub>Cl in freshwater, pH 7.0) on the mRNA expression of *rhag*, *rhbg*, *rhcg1* and *rhcg2* in the gills of *A. testudineus*. Based on the deduced amino acid sequences of Rhag, Rhbg and Rhcg2, custom-made isoform-specific antibodies were used to determine their protein abundances by western blotting, and their cellular and subcellular localization by immunofluorescence microscopy. The hypothesis tested was that environmental ammonia exposure would induce changes in the mRNA and protein expression of certain isoforms of *rhgp*/Rhgp. In addition, efforts were made to confirm

**Note on abbreviations**

In this study, two different styles were adopted for gene and protein symbols as the standard abbreviations of genes/proteins of fishes ([http://zfin.org/cgi-bin/webdriver?Mlval=aa-ZDB\\_home.app](http://zfin.org/cgi-bin/webdriver?Mlval=aa-ZDB_home.app)) are different from those of humans/non-human primates (<http://www.genenames.org>). Specifically, for fishes, gene symbols are italicized, all in lowercase, and protein designations are the same as the gene symbol, but not italicized, with the first letter in uppercase. All abbreviations were defined at the first time of usage in the text.

the existence of inwardly directed P<sub>NH<sub>3</sub></sub> and NH<sub>4</sub><sup>+</sup> concentration gradient when *A. testudineus* was exposed to 100 mmol l<sup>-1</sup> NH<sub>4</sub>Cl. We reasoned that while Rhgp could generally participate in passive ammonia excretion through pavement cells in the gills of *A. testudineus*, certain Rhgp isoforms might be involved in active NH<sub>4</sub><sup>+</sup> excretion driven by an electrical potential generated by Cl<sup>-</sup>/HCO<sub>3</sub><sup>-</sup> excretion through Cftr in specific ammonia-inducible ionocytes (Ip et al., 2012b). Because Nka  $\alpha$ -subunit 1c (Nka $\alpha$ 1c) has been proposed to be involved in active ammonia excretion (Ip et al., 2012a), it was hypothesized that certain isoforms of Rhgp would be expressed in the apical and/or basolateral membranes of the Nka $\alpha$ 1c-immunoreactive ionocytes to facilitate active NH<sub>4</sub><sup>+</sup> excretion.

**MATERIALS AND METHODS****Animals**

Specimens of *A. testudineus* (25–45 g) were purchased from a local fish distributor. Fish were maintained in dechlorinated tap water (freshwater; pH 6.8–7.0) at 25°C under a 12 h:12 h light:dark regime for 2 weeks. No attempt was made to separate the sexes. The fish were fed frozen bloodworms once every 2 days and food was withdrawn 2 days prior to the experiments. The effects of fasting have been examined in Tay et al. (2006) and were shown to have no significant effects on the nitrogen metabolism of the fish. No aeration was provided as *A. testudineus* is an obligate air-breather. Approval for the procedures adopted in this study was given by the Institutional Animal Care and Use Committee of the National University of Singapore (IACUC 021/10 and 098/10).

**Experimental conditions and sample collection**

Control fish (total *N*=11) were immersed in 25 volumes of freshwater. For exposure to environmental ammonia, fish were exposed to 100 mmol l<sup>-1</sup> NH<sub>4</sub>Cl at pH 7.0 for 1, 3 or 6 days (total *N*=21). Blood was collected through caudal puncture using a syringe coated with sodium heparin (Sigma-Aldrich, St Louis, MO, USA). The blood collected was centrifuged at 4000 *g* at 4°C for 10 min to obtain the plasma. Using an equal volume (v/v) of ice-cold 6% trichloroacetic acid, the plasma was deproteinized after centrifugation at 10,000 *g* at 4°C for 15 min and stored at -80°C. Fish were subsequently anaesthetized with an overdose of neutralized 0.05% MS-222 (Sigma-Aldrich) and killed with a strong blow to the head. Gills were quickly excised and processed for immunofluorescence microscopy or cooled in liquid nitrogen and stored at -80°C.

**Determination of plasma ammonia concentrations**

The pH of the deproteinized samples was adjusted to 6.0–7.0 with 2 mol l<sup>-1</sup> KHCO<sub>3</sub> and ammonia was assayed following the method of Bergmeyer and Beutler (1985). The change in absorbance was measured at 25°C and 340 nm using a UV-160A spectrophotometer (Shimadzu, Tokyo, Japan). Freshly prepared NH<sub>4</sub>Cl solution was used as the standard for the ammonia assay.

### mRNA extraction and cDNA synthesis

Total RNA was extracted from the gills of *A. testudineus* using Tri Reagent™ (Sigma-Aldrich) and purified using the RNeasy Plus Mini Kit (Qiagen, Hilden, Germany). The concentration of the purified total RNA was quantified spectrophotometrically using a BioSpec-nano (Shimadzu), RNA integrity was examined electrophoretically and stored at  $-80^{\circ}\text{C}$ . First-strand cDNA was synthesized from 1  $\mu\text{g}$  of total RNA using oligo(dT)<sub>18</sub> primer and the RevertAid™ first-strand cDNA synthesis kit (Thermo Fisher Scientific, Waltham, MA, USA).

### PCR

The partial sequences of *rhgp* isoforms were obtained using degenerate PCR primers (forward: 5'-TTGCCNAGBTTYAAAYTC-3'; reverse: 5'-NGCNACNCCNCCNGC-3') designed against highly conserved regions from multiple alignments of *rhgp* mRNA sequences of fish species available in GenBank (<http://www.ncbi.nlm.nih.gov/Genbank/>). PCR was carried out using the Dreamtaq™ DNA polymerase kit (Thermo Fisher Scientific), following the manufacturer's protocol. The thermal cycling conditions were  $95^{\circ}\text{C}$  (3 min), followed by 40 cycles at  $95^{\circ}\text{C}$  (30 s),  $55^{\circ}\text{C}$  (30 s),  $72^{\circ}\text{C}$  (1 min) and a final extension at  $72^{\circ}\text{C}$  (10 min). PCR products were separated electrophoretically and bands of the estimated molecular mass were excised and purified using the FavorPrep™ Gel Purification Kit (Favorgen Biotech Corporation, Ping-Tung, Taiwan).

### Cloning and sequencing of *rhgp* isoforms

The purified PCR products were cloned into pGEM®-T Easy Vector (Promega, Madison, WI, USA), transformed into JM109 cells and plated onto Luria-Bertani (LB) agar with ampicillin, X-gal and IPTG. Colonies with insert of the correct estimated size were grown overnight in LB broth with ampicillin. Plasmid extraction was performed using the AxyPrep™ Plasmid Miniprep Kit (Axygen Biosciences, Union City, CA, USA). Multiple clones of each fragment were sequenced bidirectionally using the BigDye® Terminator v3.1 Cycle Sequencing Kit (Life Technologies, Carlsbad, CA, USA), and Bioedit v7.1.3 (Hall, 1999) was used to assemble and analyze the sequences. Cloning results revealed the presence of four *rhgp* isoforms (*rhag*, *rhbg*, *rhcg1* and *rhcg2*).

### RACE-PCR

Total RNA (1  $\mu\text{g}$ ) extracted from the gills of *A. testudineus* was reverse-transcribed into 5'- and 3'-RACE-Ready cDNA with the SMARTer™ RACE cDNA Amplification Kit (Clontech Laboratories, Mountain View, CA, USA). RACE-PCR was performed using Advantage® 2 PCR Kit (Clontech Laboratories), with gene-specific primers (Table S1), to generate the cDNA fragments from the 5' and 3' ends. The thermal cycling conditions consisted of 30 cycles at  $94^{\circ}\text{C}$  (30 s),  $65^{\circ}\text{C}$  (30 s) and  $72^{\circ}\text{C}$  (4 min). The full-length cDNA was obtained by sequencing the purified RACE-PCR products bi-directionally. The complete cDNA coding sequences of *rhag*, *rhbg*, *rhcg1* and *rhcg2* have been deposited in GenBank with the respective accession numbers KF830708, KF830709, KF830710 and KF830711.

### Deduced amino acid sequences and phenogram analysis

The individual sequence of Rhag, Rhbg, Rhcg1 and Rhcg2, obtained using ExPASy proteomic server (<http://web.expasy.org/translate/>), were aligned and compared with the relevant sequences of selected animal species using Bioedit v7.1.3 (Hall, 1999). The transmembrane domains were predicted with the PSIPRED protein structure prediction server (<http://bioinf.cs.ucl.ac.uk/psipred/>) (McGuffin

et al., 2000). The sequences were aligned using ClustalX2 and phenogram analysis was performed with PHYLIP v3.6 (<http://evolution.genetics.washington.edu/phylip/doc/>) using the neighbour-joining method and 100 bootstrap replicates. Rhgp/RhGP amino acid sequences of selected animal species were obtained from GenBank or UniProtKB/TrEMBL: *Danio rerio* Rhag (AAI62203.1), *Gasterosteus aculeatus* Rhag (NP\_001254574.1), *Oncorhynchus mykiss* Rhag (ABV24962.1), *Mus musculus* RhAG (EDL23386.1), *Rattus norvegicus* RhAG (EDM18672.1), *Homo sapiens* RhAG (NP\_000315.2), *D. rerio* Rhbg (NP\_956365.2), *G. aculeatus* Rhbg (ABF69689.1), *O. mykiss* Rhbg (NP\_001118134.1), *Xenopus laevis* Rhbga (NP\_001083174.1), *X. laevis* Rhbgb (NP\_001087152.1), *X. (Silurana) tropicalis* Rhbg (NP\_001011175.1), *M. musculus* RhBG (EDL15310.1), *R. norvegicus* RhBG (EDM00730.1), *H. sapiens* RhBGa (NP\_065140.3), *H. sapiens* RhBGb (NP\_001243324.1), *H. sapiens* RhBGc (NP\_001243325.1), *D. rerio* Rhcg1 (AAM90586.1), *T. rubripes* Rhcg1 (AAM48578.1), *Lipophrys pholis* Rhcg1a (AGU71416.1), *L. pholis* Rhcg1b (AGU71417.1), *O. mykiss* Rhcg (AAU89494.1), *G. aculeatus* Rhcg (ABF69690.1), *L. pholis* Rhcg2 (AGU71418.1), *T. rubripes* Rhcg2 (AAM48579.1), *X. laevis* Rhcg (NP\_001088553.1), *X. tropicalis* Rhcg (NP\_001003661.1), *M. musculus* RhCG (AAI19046.1), *R. norvegicus* RhCG (EDM08586.1), *H. sapiens* RhCG (NP\_057405.1) and *Caenorhabditis elegans* Rhp1 (AAF97864.1) as an outgroup.

### qPCR

RNA (4  $\mu\text{g}$ ) from the gill samples of *A. testudineus* was extracted as mentioned above. The total RNA was reverse-transcribed using random hexamer primers with the RevertAid™ first-strand cDNA synthesis kit (Thermo Fisher Scientific). qPCR was performed in triplicates using a StepOnePlus™ Real-Time PCR System (Life Technologies). The PCR reactions were performed using  $2\times$  KAPA SYBR® FAST Master Mix ABI Prism® (Kapa Biosystems, Wilmington, MA, USA),  $0.3\ \mu\text{mol l}^{-1}$  forward and reverse gene-specific qPCR primers (Table S1) and 1 ng of cDNA or standard. Cycling conditions were one cycle at  $95^{\circ}\text{C}$  (20 s), followed by 40 cycles at  $95^{\circ}\text{C}$  (3 s) and  $62^{\circ}\text{C}$  (30 s). Threshold cycle ( $C_t$ ) values were collected at each elongation step and melt curve analysis was performed to verify the presence of a single product.

Absolute quantification with reference to a standard curve for each gene was adopted to determine the absolute quantity of *rhgp* transcripts in a qPCR reaction. A pure amplicon of a defined region of *rhag*, *rhbg*, *rhcg1* or *rhcg2* cDNA was produced following the PCR method of Gerwick et al. (2007). PCR was performed, as mentioned above, with the gene-specific qPCR primers (Table S1). PCR products were separated in a 2% agarose gel and purified using the FavorPrep™ Gel Purification Mini Kit (Favorgen Biotech Corporation). Sequencing was performed for the cloned purified products and quantified using a BioSpec-nano (Shimadzu).

The standard cDNA was serially diluted (from  $10^6$  to  $10^2$  copies per  $2\ \mu\text{l}$ ). A standard curve was plotted with  $C_t$  on the y-axis and the natural log of concentration on the x-axis. The PCR amplification efficiencies for *rhag*, *rhbg*, *rhcg1* and *rhcg2* were 90.4%, 99.4%, 94.5% and 93.1%, respectively. The quantity of transcript in an unknown sample was calculated from the linear regression line derived from the standard curve and expressed as copies of transcripts per nanogram total RNA.

### Western blotting

Rabbit polyclonal antibody was raised against aa 35–48 (DGKSHGHGDHGDGQS) of the translated amino acid sequence



of Rhag, against aa 449–462 (LASVRTEESEKLNS) of the translated amino acid sequence of Rhb<sub>g</sub> and against aa 388–401 (LEGNANRAGTQG) of the translated amino acid sequence of Rhcg2 (GenScript, Piscataway, NJ, USA). The rabbit polyclonal antibody for Rhcg1 (raised against aa 425–488 of *D. rerio* Rhcg1) (Nakada et al., 2007b) was kindly provided by S. Hirose (Tokyo Tech Museum and Archives, Tokyo Institute of Technology). Immunoreactive bands of Rhag, Rhb<sub>g</sub>, Rhcg1 and Rhcg2 were visualized close to the expected molecular mass of 46.8, 50.4, 53.7 and 53.0 kDa, respectively. Specificity of anti-Rhag, anti-Rhb<sub>g</sub>, anti-Rhcg1 and anti-Rhcg2 binding was validated through a peptide competition assay. The anti-Rhag (10 µg), anti-Rhb<sub>g</sub> (0.17 µg) and anti-Rhcg2 (16.65 µg) antibodies were pre-incubated with the immunizing peptide of Rhag (50 µg), Rhb<sub>g</sub> (1.7 µg) or Rhcg2 (83.25 µg) provided by Genscript, respectively, in a total volume of 200 µl at 25°C for 1 h. The 1-Step Human Coupled IVT Kit-DNA (Thermo Fisher Scientific) was used to synthesize the recombinant protein of Rhcg1 from 1 µg of the complete coding cDNA sequence of *rhcg1*, following the manufacturer's instructions. The complete coding cDNA was generated using PCR (IVT) primers (forward: 5'-GATGATAATATGGCCACCACCCATATGGGCAGCGTTC-AAAGC-3'; reverse: 5'-TTTTTTTTTTTTTTTTTTTTTCTAGT-GATCTTGATGCTCCAA-3'). The Rhcg1 recombinant protein was pre-incubated with anti-Rhcg1 at 25°C for 1 h and used for peptide competition assay.

Gill samples were homogenized three times in five volumes (w/v) of ice-cold buffer containing 50 mmol l<sup>-1</sup> of Tris HCl (pH 7.4), 1 mmol l<sup>-1</sup> of EDTA, 150 mmol l<sup>-1</sup> of NaCl, 1 mmol l<sup>-1</sup> of NaF, 1 mmol l<sup>-1</sup> of Na<sub>3</sub>VO<sub>4</sub>, 1% of NP-40, 1 mmol l<sup>-1</sup> of PMSF, and 1× HALT™ protease inhibitor cocktail (Thermo Fisher Scientific) using the pre-cooled TissueLyser LT (Qiagen) for 2.5 min at 50 Hz. The homogenate was centrifuged at 10,000 *g* for 20 min at 4°C. The protein concentration of the supernatant was determined following the method of Bradford (1976) and adjusted to 10 µg µl<sup>-1</sup> with Laemmli buffer (Laemmli, 1970). Samples were heated at 70°C for 15 min and kept at -80°C until analysis. Day 6 was chosen as the appropriate time point for the gill samples of fish exposed to 100 mmol l<sup>-1</sup> NH<sub>4</sub>Cl as the effects of the treatment condition on protein abundances would be the most representative at the final time point of the entire experiment. A total of 5 µg of gill proteins was loaded for the gel separation of Rhb<sub>g</sub>, while 50 µg of gill proteins was loaded for the gel separation of Rhag, Rhcg1 and Rhcg2. Proteins were separated by SDS-PAGE (10% acrylamide for resolving gel, 4% acrylamide for stacking gel) under conditions described in Laemmli (1970) using a vertical mini-slab apparatus (Bio-Rad Laboratories, Hercules, CA, USA). Proteins were then electrophoretically transferred onto a PVDF membrane using a transfer apparatus (Bio-Rad Laboratories). Blocking of the membrane for Rhag, Rhcg1 and actin was performed with 5% skim milk in TTBS (0.05% Tween 20 in Tris-buffered saline: 20 mmol l<sup>-1</sup> Tris-HCl, 500 mmol l<sup>-1</sup> NaCl, pH 7.6) for 1 h. Blocking of the membrane for Rhb<sub>g</sub> and Rhcg2 was performed with Pierce™ fast blocking buffer (Thermo Fisher Scientific) for 30 min. The blocked membrane was subsequently incubated with anti-Rhag antibody (1:500 dilution), anti-Rhb<sub>g</sub> antibody (1:30,000 dilution), anti-Rhcg1 antibody (1:500 dilution), anti-Rhcg2 antibody (1:300 dilution) or mouse monoclonal pan-actin antibody (Developmental Studies Hybridoma Bank, Iowa City, IA, USA; 1:500 dilution) at 25°C for 1 h. The membrane was incubated with an optimized goat anti-rabbit alkaline phosphatase-conjugated secondary antibody (Santa Cruz Biotechnology, Dallas, TX, USA) or goat anti-mouse alkaline phosphatase-conjugated

secondary antibody (Santa Cruz Biotechnology) for 1 h, rinsed with TTBS, and incubated for 30 min in a solution of 5-bromo-4-chloro-3-indolyl phosphate *p*-toluidine salt and nitro-blue tetrazolium chloride (Invitrogen, Carlsbad, CA, USA) for colour development. The developed blots were scanned using a CanonScan 9000F Mark II flatbed scanner in TIFF format at 300 dpi resolution. Densitometric quantification of band intensities was performed using ImageJ (version 1.50i, National Institutes of Health, Bethesda, MD, USA), calibrated with a 37-step reflection scanner scale (1×8 inch; Stouffer R3705-1C). Results are presented as relative protein abundance of Rhag, Rhb<sub>g</sub>, Rhcg1 or Rhcg2 normalized with actin. Brightness and contrast of the representative blots were adjusted while maintaining the integrity of the data.

### Immunofluorescence microscopy

Freshly excised gills from *A. testudineus* were immersion-fixed overnight in 3% paraformaldehyde in phosphate-buffered saline (PBS; pH 7.4) at 4°C. Samples were decalcified (30% formic acid/13% sodium citrate, pH 2.3), dehydrated in 75% ethanol and cleared in Histochoice (Sigma-Aldrich) before embedding in paraffin. Paraffin sections (5 µm) were collected on slides.

Antigen retrieval was performed by treating deparaffinized sections with 0.05% citraconic anhydride (Namimatsu et al., 2005) and blocked using 1% BSA in TPBS for 1 h. Sections were double-labelled using: (1) anti-Nkaα1c rabbit polyclonal antibody (Genscript) with anti-Nkaα1a mouse monoclonal antibody (Abmart, Shanghai, China; Ching et al., 2013) to demonstrate that Nkaα1c was not expressed in ionocytes of the freshwater control; (2) anti-NKAαRb1 rabbit polyclonal antibody [a pan-specific antibody originally designed by Ura et al. (1996)] with anti-Nkaα1b mouse monoclonal antibody (Abmart; Ching et al., 2013) to demonstrate that Nkaα1b was not expressed in ionocytes in fish exposed to ammonia; (3) anti-Nkaα1a mouse monoclonal antibody or anti-Nkaα1c mouse polyclonal antibody (Genscript) with anti-Rhag, anti-Rhb<sub>g</sub>, anti-Rhcg1 or anti-Rhcg2 rabbit polyclonal antibodies to elucidate the type of Rhgp associated with the ammonia-type ionocytes in fish exposed to ammonia; and (4) anti-CFTR mouse monoclonal antibody (Clone 24-1; R&D Systems, Minneapolis, MN, USA) with anti-Rhag to demonstrate that they can be colocalized to the apical membrane of the same ionocyte in fish exposed to ammonia.

Anti-Nkaα1a, anti-Nkaα1b, anti-Rhag, anti-Rhcg2 (1:500 dilution), anti-Nkaα1c (1:200 dilution), anti-Rhb<sub>g</sub> (1:800 dilution) and anti-Rhcg1 (1:300 dilution) were diluted in blocking buffer and incubated overnight at 4°C. Anti-CFTR (1:100 dilution) was diluted in HIKARI signal enhancer solution A (Nacalai Tesque, Kyoto, Japan) and incubated overnight at 4°C. Secondary antibody incubations using goat anti-mouse AlexaFluor® 568 and goat anti-rabbit AlexaFluor® 488 (1:500 dilution; Life Technologies) were carried out at 37°C for 1 h. After primary and secondary antibody incubations, sections were rinsed three times with TPBS and mounted in ProLong® Gold Antifade Mountant (Life Technologies). Sections were viewed on an Olympus BX60 epifluorescence microscope (Olympus, Tokyo, Japan) and images captured using the Olympus DP73 digital camera. The corresponding differential interference contrast image was captured for tissue orientation. All images were captured under predetermined optimal exposure settings. Brightness and contrast of the plates were adjusted while maintaining the integrity of the data.

### Statistical analysis

Statistical analyses were performed using SPSS v18 (IBM, Armonk, NY, USA). Normality of data and homogeneity of variance were



verified using the Shapiro–Wilk test and Levene’s test, respectively. Square-root transformation was applied for means that did not meet the assumption of normality. For means obtained from absolute quantification, one-way ANOVA (two-tailed) was performed, followed by either Tukey’s or Dunnett’s *T3 post hoc* test, depending on the homogeneity of variances. For means obtained from western blotting, an independent-samples *t*-test (two-tailed) was performed to evaluate the differences between means. Differences were regarded as statistically significant at  $P < 0.05$ .

**RESULTS**

**Nucleotides, the deduced amino acid sequences of *rhgp1***

**Rhgp and phenogram analysis**

Four *rhgp* (*rhag*, *rhbg*, *rhcg1* and *rhcg2*) were cloned from the gills of *A. testudineus*. The complete cDNA coding sequence of *rhag* consisted of 1311 bp, encoding for a protein of 437 amino acids with an estimated molecular mass of 46.8 kDa (Fig. 1). For *rhbg*, the coding sequence consisted of 1386 bp, encoding 462 amino acids

with an estimated molecular mass of 50.4 kDa (Fig. 1). In contrast, the coding sequence of *rhcg1* consisted of 1461 bp, encoding 487 amino acids with an estimated molecular mass of 53.7 kDa (Fig. 1). For *rhcg2*, the coding sequence consisted of 1446 bp, encoding 482 amino acids with an estimated molecular mass of 53.0 kDa (Fig. 1). The deduced amino acid sequences of Rhag and Rhcg2 had 12 transmembrane domains while Rhbg and Rhcg1 had 11 transmembrane domains (Figs S1–S4). A phenogram analysis of Rhag, Rhbg, Rhcg1 and Rhcg2 of *A. testudineus* revealed their close relationship to Rhag, Rhbg, Rhcg1 and Rhcg2 of teleosts, respectively, and that all four Rhgp isoforms were separated from Rhgp/RhGP of amphibians and mammals (Fig. 2).

Efforts were made to compare these sequences with EcAmtB, based on which theories of ammonia conduction by Rhgps have been formulated as its high resolution crystal structures have been resolved (Khademi et al., 2004; Zheng et al., 2004; Baday et al., 2015). Three out of the four residues crucial for  $\text{NH}_4^+$  binding (G179, H185, F235 and N236 of human RhCG) and all

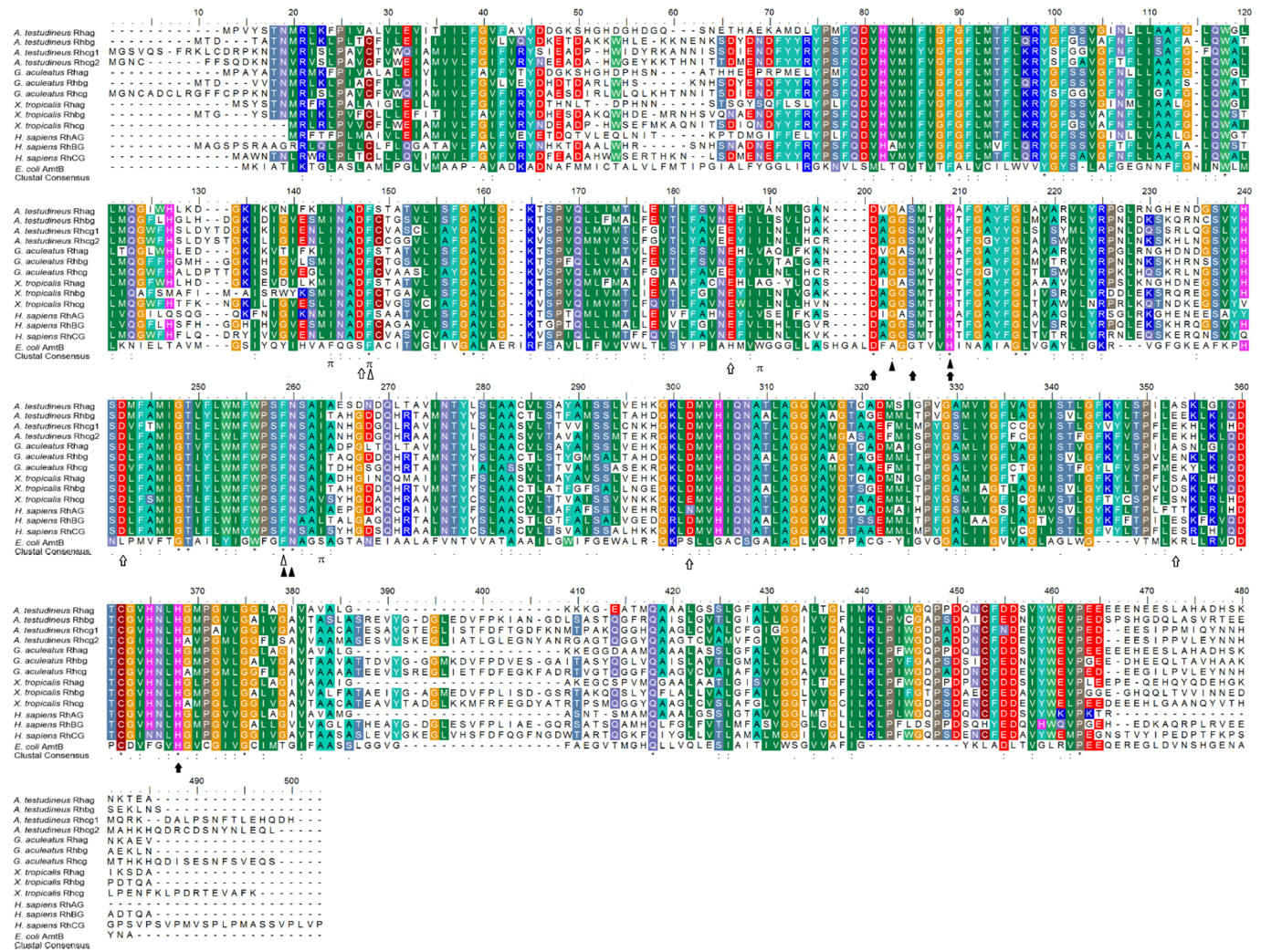


**Fig. 1. Molecular characterization of Rhesus glycoproteins (Rhgp) from the gills of *Anabas testudineus*.** Multiple amino acid alignment of Rhag, Rhbg, Rhcg1 and Rhcg2 from the gills of *A. testudineus*, with known Rhgp/RhGP isoforms from *Gasterosteus aculeatus* (Rhag: ABF69688.1, Rhbg: ABF69689.1, Rhcg: ABF69690.1), *Xenopus (Silurana) tropicalis* (Rhag: NP\_001039257.1, Rhbg: NP\_001011175.1, Rhcg: NP\_001003661.1), *Homo sapiens* (RhAG: NP\_000315.2, RhBG: NP\_065140.3, RhCG: NP\_057405.1) and *Escherichia coli* ammonia transporter (AmtB: NP\_414985.1). Identical amino acid residues are indicated by asterisks, strongly similar amino acids are indicated by colons and weakly similar amino acids are indicated by periods. Residues involved in  $\text{NH}_4^+$  binding or deprotonation of  $\text{NH}_4^+$  for  $\text{NH}_3$  conduction are indicated by shaded triangles and arrows, respectively. The phenylalanine gate and the acidic residues important for  $\text{NH}_3$  permeation are indicated by open triangles and arrows, respectively. The  $\pi$ -cation binding sites of *E. coli* AmtB are denoted with  $\pi$ .

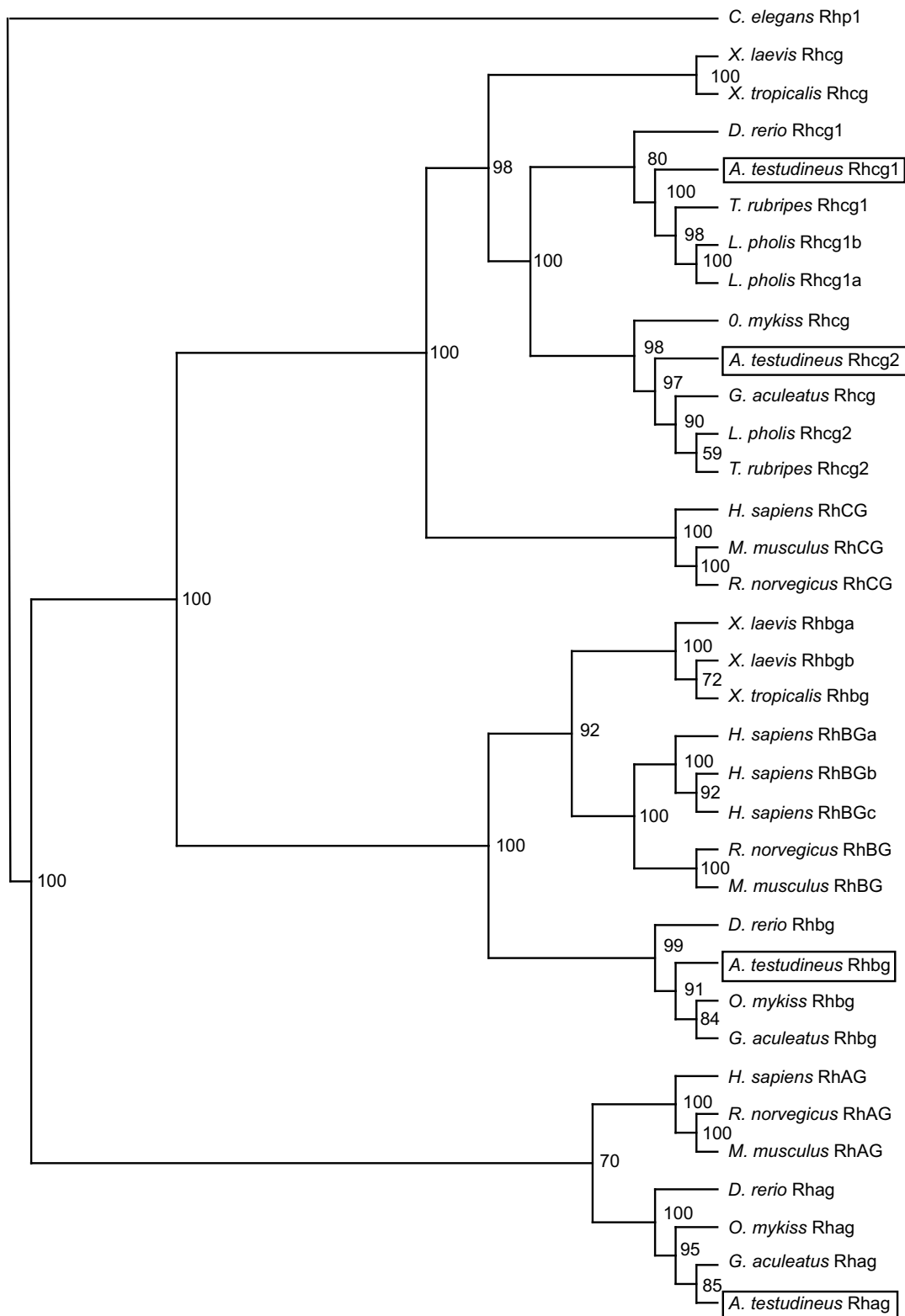


**Fig. 2. Phenogram analysis of Rhesus glycoproteins (Rhgp) from the gills of *Anabas testudineus*.** A phenogram illustrating the amino acid sequence similarities and the relationship between Rhag, Rhbg, Rhcg1 and Rhcg2 from the gills of *A. testudineus* and Rhgp/RhGP of selected vertebrates. Numbers presented at each branch point represent bootstrap values from 100 replicates. *Caenorhabditis elegans* Rhp1 is used as an outgroup for the phenogram.

amino acid residues involved in the deprotonation of  $\text{NH}_4^+$  for  $\text{NH}_3$  conduction (D177, S181, H185 and H344 of human RhCG) were conserved in the Rhgps of *A. testudineus* (Fig. 1). However, in all four Rhgp sequences of *A. testudineus*, three of the four

amino acid residues (F103, F107, W148 and S219 of *E. coli* AmtB), which form the  $\pi$ -cation binding sites, were replaced with smaller non-polar aliphatic amino acids (F103I, W148V and S219I) (Fig. 1).

Five acidic amino acid residues, D129, E166, D218, D278 and E329, lined the extracellular and intracellular vestibules of human RhCG (Gruswitz et al., 2010). With the exception of an amino acid substitution (E329A) in Rhag, these amino acids were well conserved in all the four Rhgp sequences examined. In addition, two phenylalanine residues (F130 and F235 of human RhCG) responsible for gating of the channel were conserved in all four *A. testudineus* Rhgp sequences.

#### mRNA expression of *rhgp* in the gills of fish exposed to 100 mmol l<sup>-1</sup> NH<sub>4</sub>Cl

When compared with the freshwater control, the mRNA expression level of *rhag* increased significantly in the gills of *A. testudineus* exposed to 100 mmol l<sup>-1</sup> NH<sub>4</sub>Cl for 1 day (by 1.4-fold) and decreased significantly after 6 days (by 47%) of ammonia exposure (Fig. 3A). The mRNA expression level of *rhbg*, in contrast, increased significantly after 1 day (by 1.9-fold) or 3 days (by 1.7-fold) of ammonia exposure before returning to the control level on day 6 (Fig. 3B). By contrast, the mRNA expression level of *rhcg1* increased significantly after 6 days (by 1.7-fold) of ammonia exposure (Fig. 3C). There was a significant increase in the mRNA expression level of *rhcg2* in the gills of fish exposed to ammonia for 1 day (by 24.0-fold) or 3 days (by 5.7-fold), but the *rhcg2* transcript level returned to control levels on day 6 of ammonia exposure (Fig. 3D).

#### Protein abundances of Rhgp in the gills of fish after 6 days of exposure to 100 mmol l<sup>-1</sup> NH<sub>4</sub>Cl

The protein abundances of Rhag and Rhcg2 increased significantly (by 1.51-fold and 2.4-fold, respectively) in the gills of fish exposed to ammonia for 6 days, but those of Rhbg and Rhcg1 remained unchanged after 6 days of ammonia exposure (Fig. 4). The specificity of antibody binding was verified through a peptide competition assay (Fig. S5).

#### Immunofluorescent localization of Rhgp with Nkaα1a or Nkaα1c in the gills of fish after 6 days of exposure to 100 mmol l<sup>-1</sup> NH<sub>4</sub>Cl

The freshwater-type ionocytes expressed Nkaα1a but not Nkaα1c (Fig. 5A). In comparison, the gills of fish exposed to 100 mmol l<sup>-1</sup> NH<sub>4</sub>Cl for 6 days expressed both Nkaα1a- and Nkaα1c-immunoreactive ionocytes (Fig. 5B). The copy number of *nkaα1b* transcripts is very low (<40 copies per nanogram cDNA) within the gills of the ammonia-exposed fish (Ip et al., 2012a), and thus Nkaα1b is unlikely to be physiologically significant during environmental ammonia exposure. Because the gills of the ammonia-exposed *A. testudineus* expressed Nkaα1a and Nkaα1c but not Nkaα1b (Fig. 5B,C), samples were double-labelled with anti-Rhgp and anti-Nkaα1a or anti-Nkaα1c to identify the types of ionocytes involved in ammonia excretion and to characterize the subcellular localization of Rhgp. For fish kept in freshwater, while there were branchial epithelial cells that expressed only Nkaα1a or epithelial cells and erythrocytes that expressed only Rhag, Rhag immunofluorescence was detected in the apical membrane of some Nkaα1a-labelled ionocytes along the secondary lamellae (Fig. 6A). By contrast, in the gills of fish exposed to ammonia, Rhag was localized to the apical membrane of not only certain Nkaα1a-labelled ionocytes but also some Nkaα1c-labelled ionocytes (Fig. 6B,C), with more cells (including erythrocytes) expressing only Rhag shown in Fig. 6B compared with Fig. 6C. None of the Nkaα1a- and Nkaα1c-labelled ionocytes expressed Rhbg, and the anti-Rhbg antibody appeared to label some special membranes inside the secondary lamellae (Fig. 7).

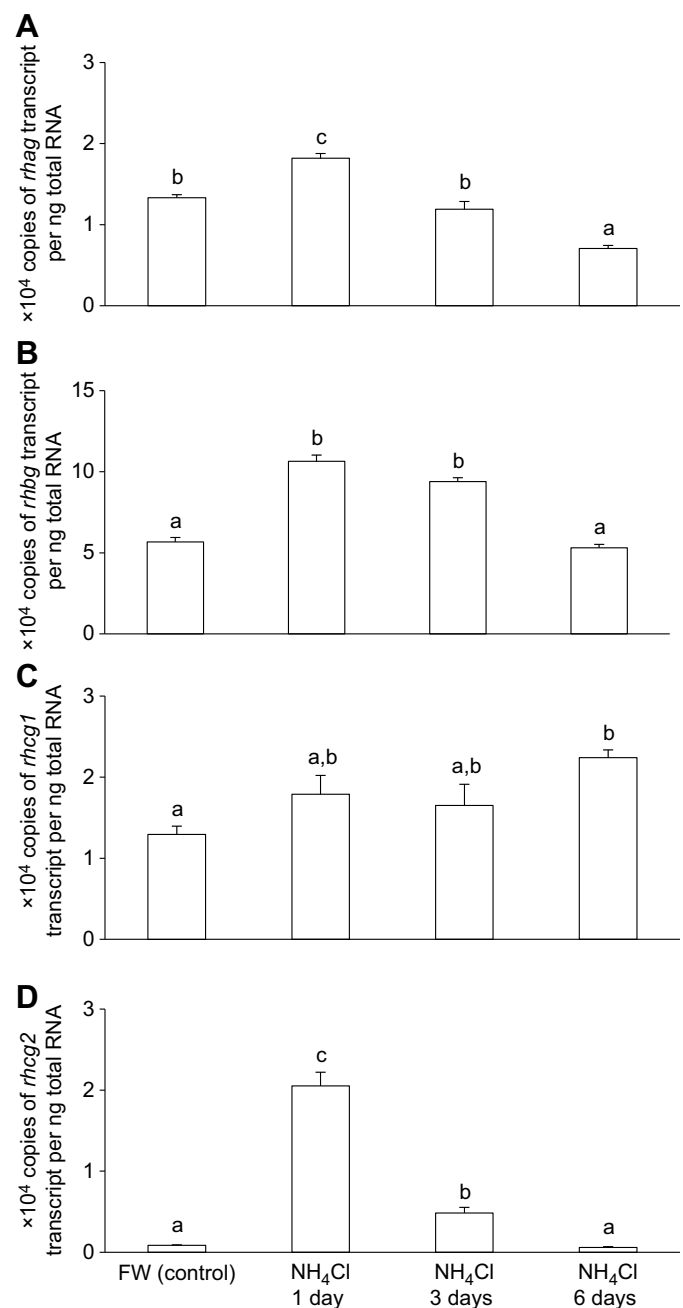


**Fig. 3.** mRNA expression levels of *rhesus glycoprotein (rhgp)* in the gills of *Anabas testudineus* exposed to environmental ammonia. Absolute quantification (copies of transcript per ng total RNA) of (A) *rhesus blood group-associated glycoprotein (rhag)*, (B) *rhesus family B glycoprotein (rhbg)*, (C) *rhesus family C glycoprotein 1 (rhcg1)* or (D) *rhesus family C glycoprotein 2 (rhcg2)* transcripts in the gills of *A. testudineus* kept in freshwater (FW; control) or after 1, 3 or 6 days of exposure to 100 mmol l<sup>-1</sup> NH<sub>4</sub>Cl. Results represent means ± s.e.m. (N=4). Means not sharing the same letter are significantly different (P<0.05).

Rhcg1 labelling was detected along the secondary lamellae of the gills of the control fish in freshwater, but Rhcg1 was not associated with the Nkaα1a-labelled ionocytes (Fig. 8A). Similarly, no Rhcg1 expression in the Nkaα1a- or Nkaα1c-labelled ionocytes was observed in the gills of the ammonia-exposed fish (Fig. 8B,C). For the freshwater control, double-labelling of anti-Rhcg2 (green) with anti-Nkaα1a (red) produced a yellow-orange colour, denoting



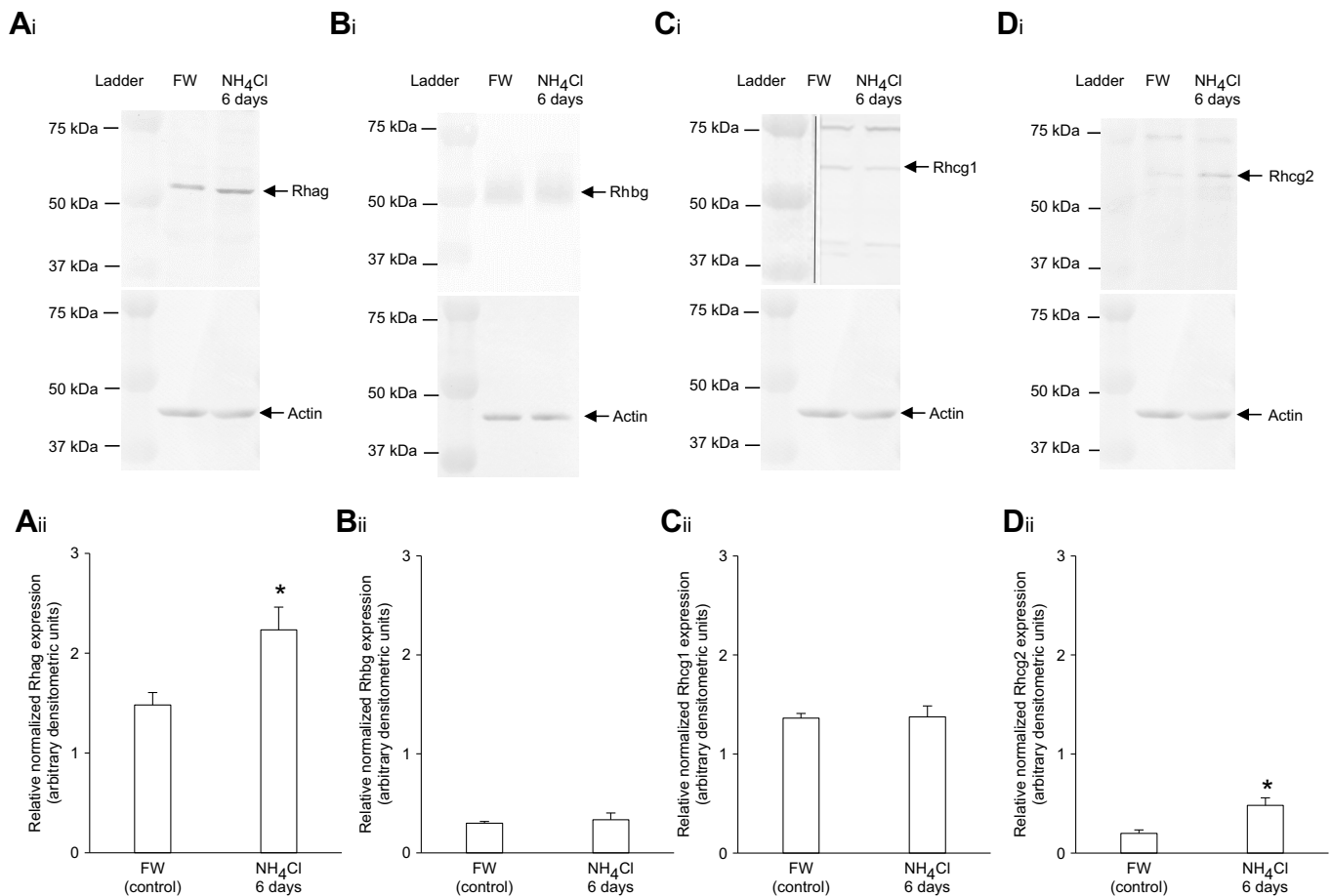


**Fig. 4. Western blotting results of Rhesus glycoprotein (Rhgp) in the gills of *Anabas testudineus* exposed to environmental ammonia.** Protein abundance of (A) Rhesus blood group-associated glycoprotein (Rhag), (B) Rhesus family B glycoprotein (Rhbg), (C) Rhesus family C glycoprotein 1 (Rhcg1) and (D) Rhesus family C glycoprotein 2 (Rhcg2) in the gills of *A. testudineus* kept in freshwater (FW; control) or after 6 days of exposure to 100 mmol l<sup>-1</sup> NH<sub>4</sub>Cl. (i) An example of an immunoblot of Rhag, Rhbg, Rhcg1 or Rhcg2 and actin. (ii) The protein abundance of Rhag, Rhbg, Rhcg1 or Rhcg2 normalized with respect to actin. Results represent means±s.e.m. (*N*=3). Asterisks indicate a significant difference from the corresponding freshwater control (*P*<0.05). Because of interaction of anti-Rhcg1 with the ladder, the lane containing the ladder was cut out prior to primary antibody incubation and pieced together with the rest of the membrane before scanning. Both the ladder and protein samples were electrophoresed concurrently on the same gel. Site of splicing for Ci is denoted by a black line.

that Rhcg2 and Nkaα1a were co-localized to the basolateral membranes of ionocytes in the secondary lamellae (Fig. 9A). Additionally, Rhcg2 and Nkaα1a were co-localized to the basolateral membranes of the Nkaα1a-labelled ionocytes in the ammonia-exposed fish, with the exception of a few cells that expressed only Rhcg2 and not Nkaα1a (Fig. 9B). In addition, Rhcg2 was expressed in the basolateral membranes of some Nkaα1c-labelled ionocytes in the gills of fish exposed to ammonia (Fig. 9C). This is the first report on the expression of Rhcg2 in two different types of branchial ionocytes in response to ammonia exposure.

#### Immunofluorescent localization of Rhag with Cfr in the gills of fish after 6 days of exposure to 100 mmol l<sup>-1</sup> NH<sub>4</sub>Cl

Both Rhag and Cfr were co-expressed on the apical membranes of ionocytes in the secondary lamellae of gills of fish exposed to ammonia (Fig. 6D).

#### Plasma ammonia concentration

The plasma ammonia concentration of *A. testudineus* kept in freshwater was 0.18±0.04 mmol l<sup>-1</sup> (*N*=4). After 6 days of exposure to 100 mmol l<sup>-1</sup> NH<sub>4</sub>Cl, the plasma ammonia concentration increased significantly to 2.4±0.3 mmol l<sup>-1</sup> (*N*=4).

## DISCUSSION

### Molecular characterization of Rhgp from gills of *A. testudineus*

Amino acid residues involved in (1) NH<sub>4</sub><sup>+</sup> binding, (2) gating of the channels, (3) deprotonation of NH<sub>4</sub><sup>+</sup> and (4) lining of the channel vestibules (Khademi et al., 2004; Zheng et al., 2004; Baday et al., 2015) are conserved in these four Rhgp of *A. testudineus*, indicating that they can function as ammonia transporters in the gills. In human RhCG, acidic residues D129, E166, D218, D278 and E329 lining the extracellular and intracellular vestibules may play a role in NH<sub>4</sub><sup>+</sup> binding (Gruswitz et al., 2010), and four of these acidic residues (all except E329) were conserved in the four Rhgp of *A. testudineus*. Other crucial amino acid residues that provide high affinity and selectivity for NH<sub>4</sub><sup>+</sup> include W148 and S219, both of which form the π-cation binding site in AmtB (Khademi et al., 2004; Zheng et al., 2004). In EcAmtB, W148 serves to recruit NH<sub>4</sub><sup>+</sup> via cation attractions to their π electrons while S219 facilitates this process through hydrogen bonding with NH<sub>4</sub><sup>+</sup>. Fong et al. (2007) demonstrated that W148L substitution in EcAmtB increased the flux of NH<sub>4</sub><sup>+</sup> and CH<sub>3</sub>NH<sub>3</sub><sup>+</sup> by enlarging the opening of EcAmtB pore. As W148 is substituted with smaller, non-polar amino acids such as leucine, valine or isoleucine in the four Rhgp of *A. testudineus*, the possibility of NH<sub>4</sub><sup>+</sup> permeation cannot be ignored.

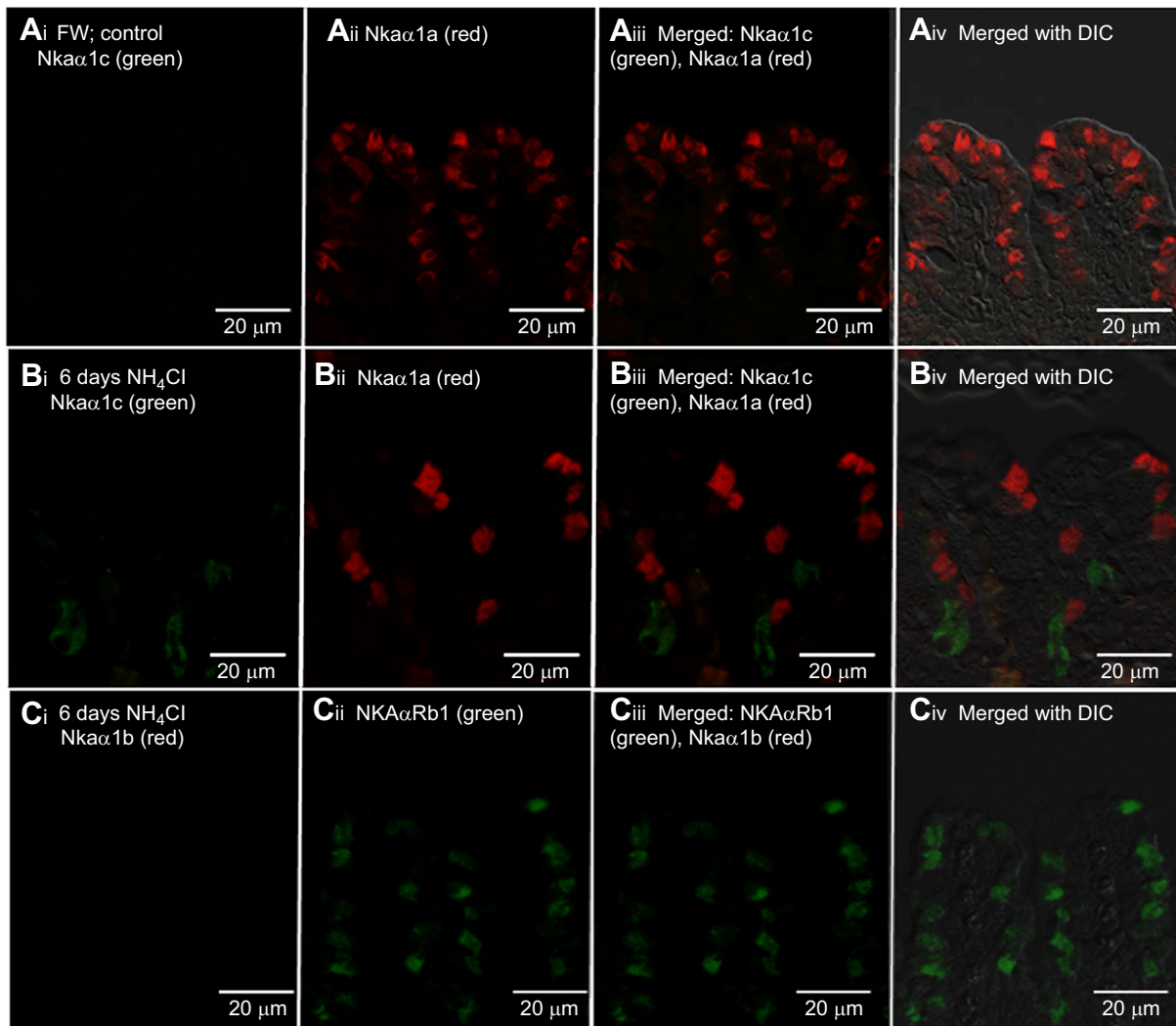


**Fig. 5. Immunofluorescent localization of  $\text{Na}^+/\text{K}^+$ -ATPase (Nka)  $\alpha$ -subunits in the gills of *Anabas testudineus*.** Double immunofluorescence was performed on the gills of *A. testudineus* (A) in freshwater (FW; control) using anti-Nka $\alpha$ 1c and anti-Nka $\alpha$ 1a antibodies, or after 6 days of exposure to  $100 \text{ mmol l}^{-1}$   $\text{NH}_4\text{Cl}$  using (B) anti-Nka $\alpha$ 1c and anti-Nka $\alpha$ 1a antibodies or (C) anti-Nka $\alpha$ 1b and anti-Nka $\alpha$ Rb1 antibodies. Immunofluorescence of anti-Nka $\alpha$ 1c (green) or anti-Nka $\alpha$ 1b (red) and anti-Nka $\alpha$ 1a (red) or anti-Nka $\alpha$ Rb1 (green) antibodies are shown in i and ii, respectively. Both channels (green and red) are merged in iii and overlaid with differential interference contrast (DIC) image for orientation in iv. Magnification: 400 $\times$ .

Two phenylalanine residues at positions 107 and 215 of EcAmtB may be involved in gating of the channel (Zheng et al., 2004). In human RhCG, these two residues correspond to F130 and F235 (Gruswitz et al., 2010), and a mutation of F235V results in reduced ammonia transport (Zidi-Yahiaoui et al., 2006). These two phenylalanine residues are conserved in all four Rhgp of *A. testudineus*. Two histidine residues (H168 and H318 corresponding to H185 and H344 in human RhCG, respectively) located in the midpoint of the ammonia conduction pore of EcAmtB may participate in the deprotonation of  $\text{NH}_4^+$ , releasing electroneutral  $\text{NH}_3$ , which permeates the largely hydrophobic channel (Khademi et al., 2004). These two histidine residues are present in the four Rhgp of *A. testudineus*. However, it has been reported recently that the deprotonation role assigned to these two histidine residues may not be necessary, as demonstrated by the triple mutants H168D/H318D/I110N and H168D/H318E/I110N of EcAmtB (Hall and Kustu, 2011). Notwithstanding the assertion that two histidine residues are involved in the deprotonation of  $\text{NH}_4^+$ , a single change of H168 or H318 to alanine also does not eradicate ammonia transport in ammonia-dependent yeast strains (Wang et al., 2013).

Taken together, the deprotonation of  $\text{NH}_4^+$  and a hydrophobic pore are not absolute requirements for ammonia transport, implying that  $\text{NH}_4^+$ , instead of  $\text{NH}_3$ , could be the permeating ammonia species (Loqué et al., 2009; Hall and Kustu, 2011).

#### Rhgp and passive ammonia excretion in fish gills

In fishes, it has been generally accepted that ammonia is excreted mainly as  $\text{NH}_3$  down a favorable blood-to-water diffusion gradient, and  $\text{NH}_3$  excretion is facilitated through  $\text{NH}_3$  trapping by  $\text{H}^+$  excreted through apical  $\text{Na}^+/\text{H}^+$  exchangers and/or  $\text{H}^+$ -ATPases (Wilkie, 1997, 2002; Evans et al., 2005; Weihrauch et al., 2009; Wright and Wood, 2009; Ip and Chew, 2010). Moreira-Silva et al. (2010) reported that  $\text{H}^+$ -ATPase and Rhcg1 were co-localized to a type of cell that is not rich in Nka in the gills of the weatherloach, *Misgurnus anguillicaudatus*. Treatment with bafilomycin decreased ammonia excretion in *M. anguillicaudatus*, which supports  $\text{H}^+$ -ATPase being involved in  $\text{NH}_3$  trapping. However, in some species such as *Oryzias latipes*,  $\text{Na}^+/\text{H}^+$  exchanger 3 and Rhcg1 were colocalized to a group of ionocytes in the embryos, and ammonia excretion was blocked by 5-(N-ethyl-N-isopropyl) amiloride, which

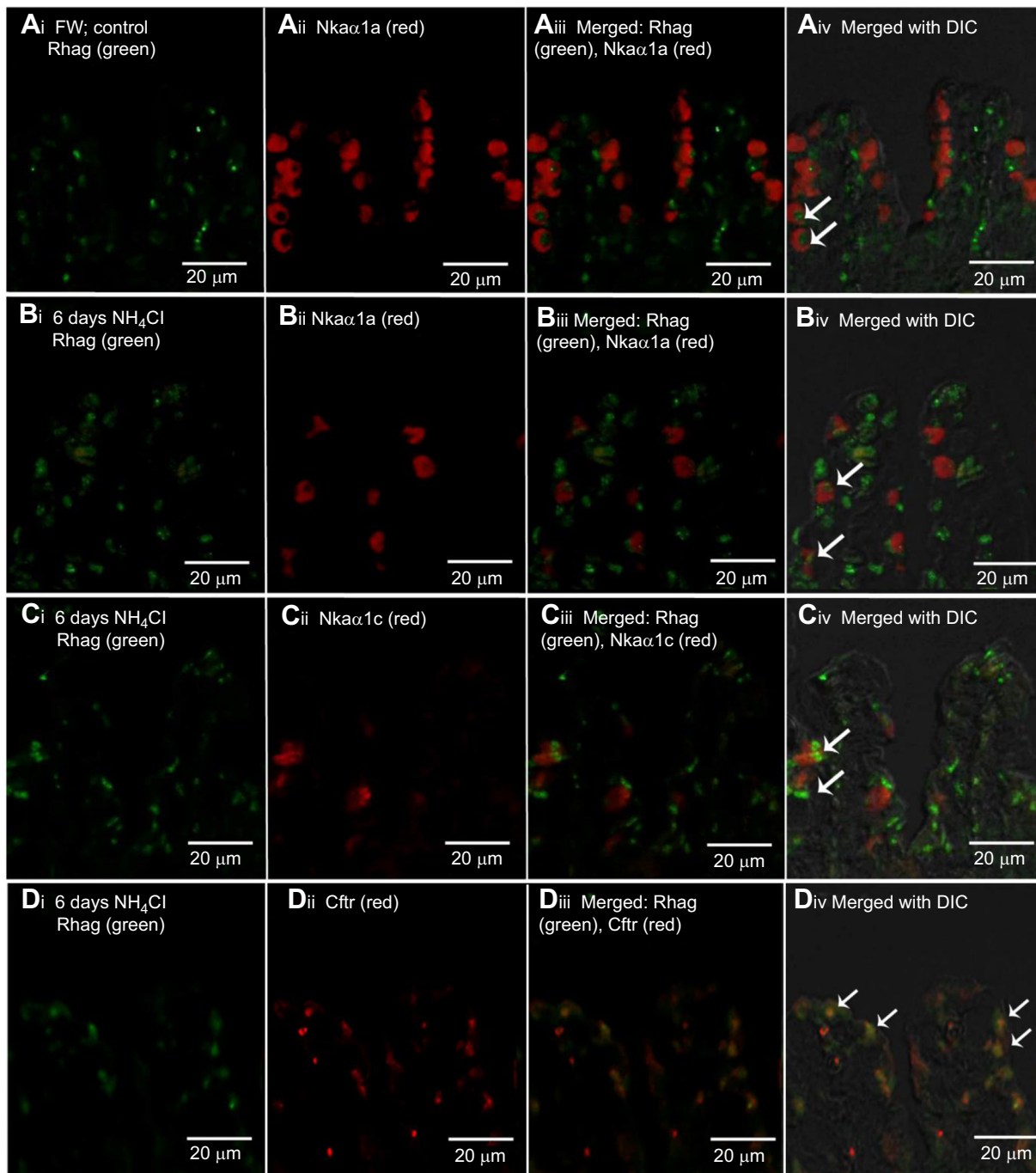


**Fig. 6. Immunofluorescent localization of Rhesus blood group-associated glycoprotein (Rhag) and  $\text{Na}^+/\text{K}^+$ -ATPase  $\alpha 1\text{a}$  ( $\text{Nka}\alpha 1\text{a}$ ),  $\text{Nka}\alpha 1\text{c}$  or cystic fibrosis transmembrane conductance regulator  $\text{Cl}^-$  channel (Cfr) in the gills of ammonia-exposed *Anabas testudineus*.** Double immunofluorescence was performed on the gills of *A. testudineus* (A) kept in freshwater (FW; control) using anti-Rhag and anti- $\text{Nka}\alpha 1\text{a}$  antibodies, or after 6 days of exposure to  $100 \text{ mmol l}^{-1} \text{ NH}_4\text{Cl}$  using (B) anti-Rhag and anti- $\text{Nka}\alpha 1\text{a}$  antibodies, (C) anti-Rhag and anti- $\text{Nka}\alpha 1\text{c}$  antibodies or (D) anti-Rhag and anti-CFR antibodies. Immunofluorescence of anti-Rhag (green) and anti- $\text{Nka}\alpha 1\text{a}$ , anti- $\text{Nka}\alpha 1\text{c}$  or anti-CFR (red) antibodies are shown in i and ii, respectively. Both channels (green and red) are merged in iii and overlaid with DIC image for orientation in iv. Arrows in Aiv, Biv and Civ indicate the apical localization of Rhag while arrows in Div indicate apical localization of Rhag and Cfr. Magnification:  $400\times$ .

is a specific inhibitor of  $\text{Na}^+/\text{H}^+$  exchanger, but not bafilomycin, suggesting that the  $\text{Na}^+/\text{H}^+$  exchanger plays an important role in ammonia excretion (Wu et al., 2010). It has been proposed for fish gills that Rhag mediates the transport of  $\text{NH}_3$  from erythrocytes, Rhbg transports  $\text{NH}_3$  across the basolateral membrane of ionocytes, and a metabolon comprising several ion transporters (Rhcg1,  $\text{H}^+$ -ATPase,  $\text{Na}^+/\text{H}^+$  exchanger and epithelial  $\text{Na}^+$  channel) provides an

acid-trapping mechanism for apical  $\text{NH}_3$  excretion (Wright and Wood, 2009).

#### Active $\text{NH}_4^+$ excretion in *A. testudineus* during ammonia exposure

At pH 7.0, a solution of  $100 \text{ mmol l}^{-1} \text{ NH}_4\text{Cl}$  contained  $99.1$  and  $0.91 \text{ mmol l}^{-1}$  of  $\text{NH}_4^+$  and  $\text{NH}_3$ , respectively. Taking the plasma



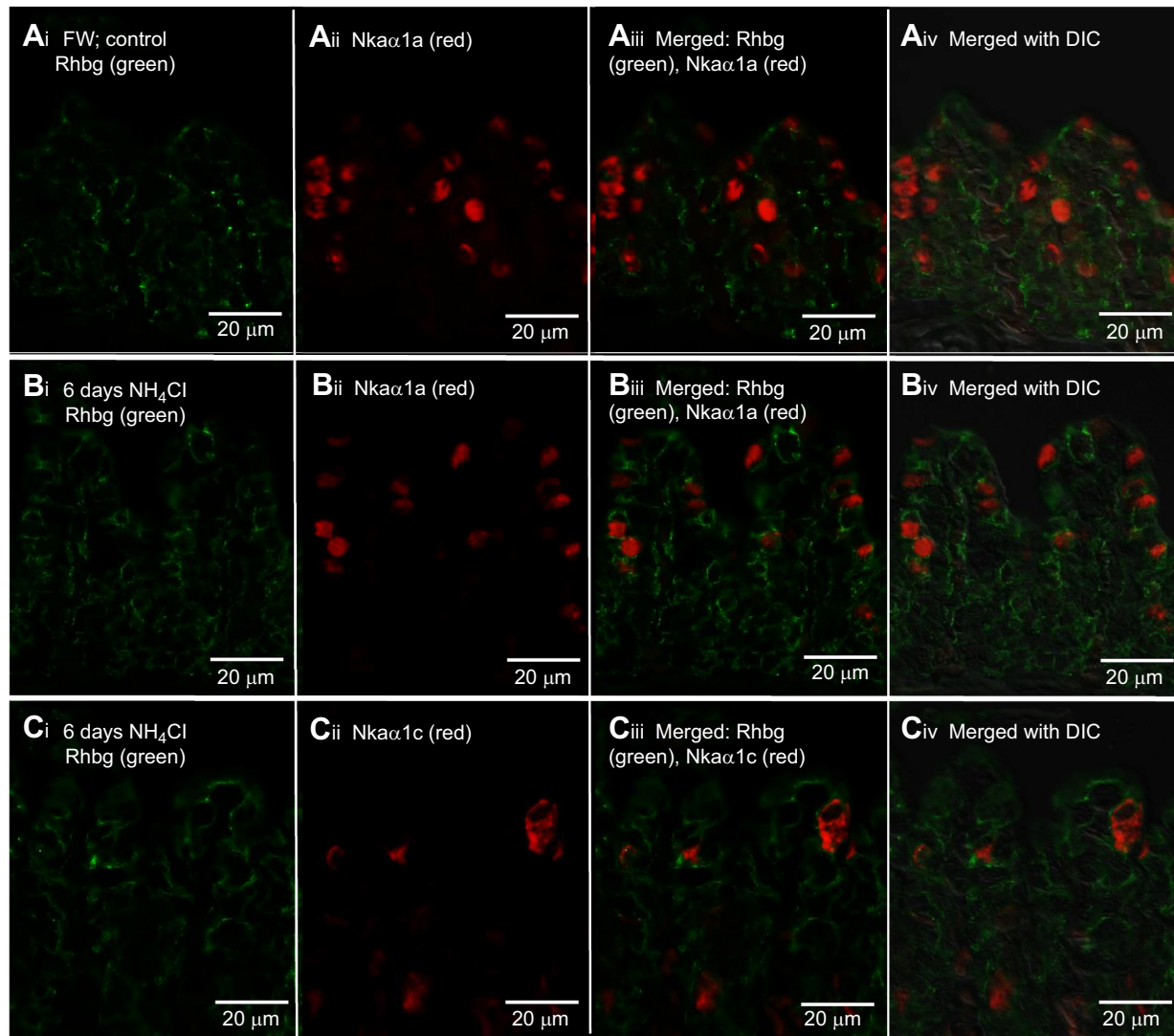


**Fig. 7. Immunofluorescent localization of Rhesus family B glycoprotein (Rhbg) and  $\text{Na}^+/\text{K}^+$ -ATPase  $\alpha 1\text{a}$  ( $\text{Nka}\alpha 1\text{a}$ ) or  $\text{Nka}\alpha 1\text{c}$  in the gills of ammonia-exposed *Anabas testudineus*.** Double immunofluorescence was performed on the gills of *A. testudineus* (A) kept in freshwater (FW; control) using anti-Rhbg and anti- $\text{Nka}\alpha 1\text{a}$  antibodies, or after 6 days of exposure to  $100 \text{ mmol l}^{-1} \text{ NH}_4\text{Cl}$  using (B) anti-Rhbg and anti- $\text{Nka}\alpha 1\text{a}$  antibodies or (C) anti-Rhbg and anti- $\text{Nka}\alpha 1\text{c}$  antibodies. Immunofluorescence of anti-Rhbg (green) and anti- $\text{Nka}\alpha 1\text{a}$  or anti- $\text{Nka}\alpha 1\text{c}$  (red) antibodies are shown in i and ii, respectively. Both channels (green and red) are merged in iii and overlaid with DIC image for orientation in iv. Magnification:  $400\times$ .

pH as 7.6 (Ip et al., 2012b), the plasma  $\text{NH}_4^+$  and  $\text{NH}_3$  concentrations of *A. testudineus* exposed to  $100 \text{ mmol l}^{-1} \text{ NH}_4\text{Cl}$  for 6 days were estimated to be 2.25 and  $0.15 \text{ mmol l}^{-1}$ , respectively. Hence, *A. testudineus* was confronted with steep, inwardly directed gradients of  $\text{NH}_4^+$  and  $\text{NH}_3$ , conditions under which many fishes would succumb within minutes owing to the impediment of ammonia excretion and a net influx of ammonia from the environment (Chew and Ip, 2014). By contrast, *A. testudineus* can obviously maintain a low plasma ammonia concentration by excreting ammonia actively against unfavorable blood-to-water  $\text{NH}_4^+$  and  $\text{NH}_3$  gradients (Tay et al., 2006; Ip et al., 2012b). However, unlike other fish species, *A. testudineus* alkalizes the external medium and decreases bafilomycin-sensitive branchial  $\text{H}^+$ -ATPase activity during exposure to high concentrations of environmental ammonia (Ip et al., 2012b). Hence,  $\text{NH}_3$  trapping by  $\text{H}^+$ , as suggested for other fishes (Wright and Wood, 2009), does not appear to be the driving force behind the movement of ammonia against unfavorable  $\text{P}_{\text{NH}_3}$  and  $\text{NH}_4^+$

gradients in the gills of *A. testudineus*, and some other mechanism(s), e.g. Cftr (Ip et al., 2012b), must be working in collaboration with certain putative ammonia transporters.

#### **Ammonia exposure leads to changes in transcript and protein levels of *rhgp/Rhgp* in the gills of *A. testudineus***

Environmental ammonia exposure triggers an upregulation of *rhgp* mRNA expression in embryos and larvae of zebrafish (Braun et al., 2009a), and the gills of pufferfish (Nawata et al., 2010), mangrove killifish (Hung et al., 2007) and rainbow trout (Nawata et al., 2007; Wood and Nawata, 2011), but these fishes are not known to actively excrete ammonia. For rainbow trout, ammonia infusion results in a rise in plasma ammonia concentration, upregulation in mRNA expression levels of branchial *rhbg* and *rhcg2*, and an increase in ammonia excretion rate (Nawata and Wood, 2009). Furthermore, exposure of cultured trout gill cells to ammonia results in an upregulation in the mRNA expression of *rhbg* and *rhcg2* (Tsui et al., 2009). Unlike the fishes mentioned above, it is probable that active

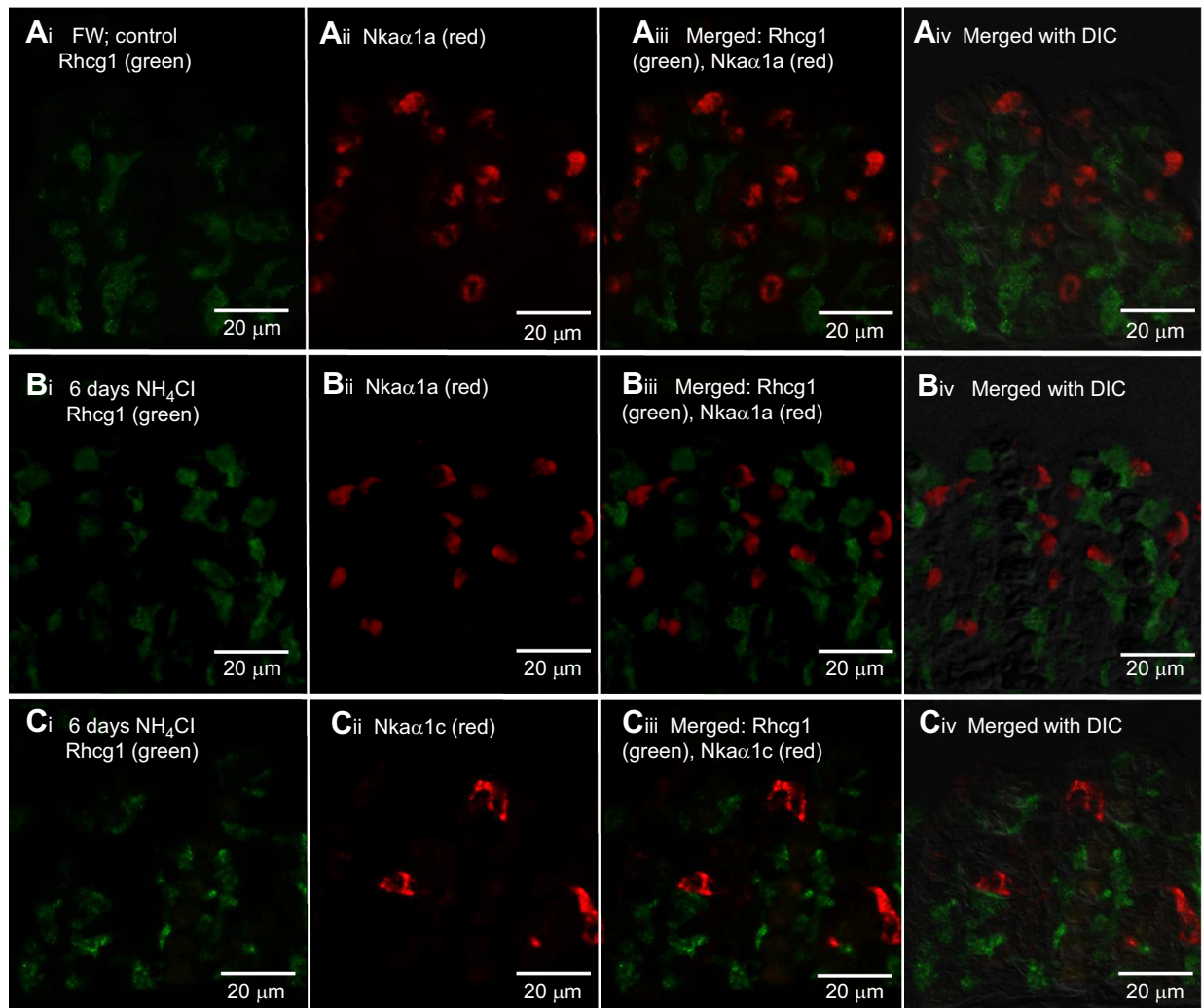


**Fig. 8.** Immunofluorescent localization of Rhesus family C glycoprotein 1 (Rhcg1) and  $\text{Na}^+/\text{K}^+$ -ATPase  $\alpha 1a$  (Nka $\alpha 1a$ ) or Nka $\alpha 1c$  in the gills of ammonia-exposed *Anabas testudineus*. Double immunofluorescence was performed on the gills of *A. testudineus* (A) kept in freshwater (FW; control) using anti-Rhcg1 and anti-Nka $\alpha 1a$  antibodies, or after 6 days of exposure to  $100 \text{ mmol l}^{-1} \text{ NH}_4\text{Cl}$  using (B) anti-Rhcg1 and anti-Nka $\alpha 1a$  antibodies or (C) anti-Rhcg1 and anti-Nka $\alpha 1c$  antibodies. Immunofluorescence of anti-Rhcg1 (green) and anti-Nka $\alpha 1a$  or anti-Nka $\alpha 1c$  (red) antibodies are shown in i and ii, respectively. Both channels (green and red) are merged in iii and overlaid with DIC image for orientation in iv. Magnification: 400 $\times$ .

ammonia excretion through the gills of *A. testudineus* necessitates the upregulation of certain type(s) of ammonia transporter in association with a specific type of branchial ionocyte during ammonia exposure. Indeed, there were significant increases in the mRNA expression levels of *rhag*, *rhbg*, *rhcg1* and *rhcg2* in the gills of *A. testudineus* at specific time points during the 6 days of ammonia exposure, with significant increases in the protein abundances of Rhag and Rhcg2 on day 6. These results confirm that ammonia exposure can induce transcriptional and translational changes to *rhgp*/Rhgp expression in the gills of *A. testudineus*. It is apparent that changes in transcription preceded changes in translation for *rhag*/Rhag and *rhcg2*/Rhcg2, as transcript levels decreased or returned to normal on day 6, when the required increase in protein abundance had been achieved. While Rhbg and Rhcg2 appear to be the key players in passive branchial ammonia excretion when plasma ammonia levels are elevated in the freshwater rainbow trout (Nawata and Wood, 2009), active ammonia excretion through the gills of *A. testudineus* apparently involves Rhag and Rhcg2, as indicated by their increased protein abundance in response to environmental ammonia exposure. Rhbg

and Rhcg1 are unlikely to be involved in active ammonia excretion in *A. testudineus*. Despite transient increases in their branchial mRNA expression levels, there were no significant changes in their protein abundance after 6 days of ammonia exposure, but active ammonia excretion would have occurred. Even though we cannot eliminate the possibility of a significant increase in the protein abundance of Rhbg and Rhcg1 before 6 days of ammonia exposure, its return to control levels on the sixth day suggests that they were unlikely to be involved in active ammonia excretion. More importantly, Rhbg and Rhcg1 were not expressed in ionocytes; they were localized separately in disparate non-Nka-immunoreactive cells in the gills of the control fish and fish exposed to ammonia. In rainbow trout and pufferfish, Rhbg and Rhcg2 are expressed in pavement cells to facilitate passive ammonia excretion (Nawata et al., 2007; Nakada et al., 2007a). Therefore, it is probable that Rhbg or Rhcg1 could be expressed in pavement cells of *A. testudineus* to support ammonia excretion under normal circumstances or when exposed to low concentrations of environmental ammonia. However, during the early phase of exposure to supposedly ammonia-loading conditions, the gills

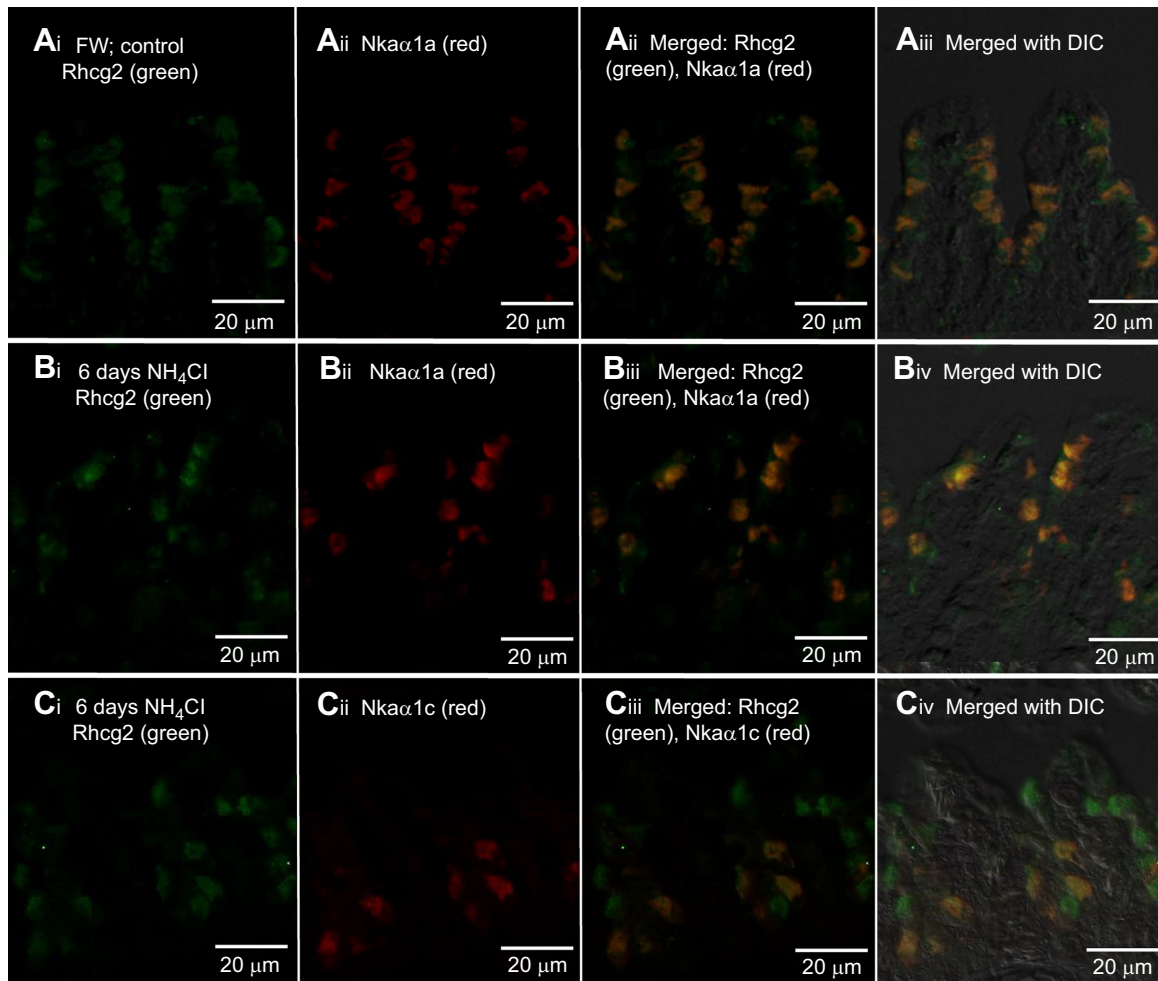


**Fig. 9. Immunofluorescent localization of Rhesus family C glycoprotein 2 (Rhcg2) and  $\text{Na}^+/\text{K}^+$ -ATPase  $\alpha 1\text{a}$  (Nka $\alpha 1\text{a}$ ) or Nka $\alpha 1\text{c}$  in the gills of ammonia-exposed *Anabas testudineus*.** Double immunofluorescence was performed on the gills of *A. testudineus* kept in (A) freshwater (FW; control) using anti-Rhcg2 and anti-Nka $\alpha 1\text{a}$  antibodies, or after 6 days of exposure to  $100 \text{ mmol l}^{-1} \text{ NH}_4\text{Cl}$  using (B) anti-Rhcg2 and anti-Nka $\alpha 1\text{a}$  antibodies or (C) anti-Rhcg2 and anti-Nka $\alpha 1\text{c}$  antibodies. Immunofluorescence of anti-Rhcg2 (green) and anti-Nka $\alpha 1\text{a}$  or anti-Nka $\alpha 1\text{c}$  (red) antibodies are shown in i and ii, respectively. Both channels (green and red) are merged in iii and overlaid with DIC image for orientation in iv. Co-localization of staining from the green and red channels resulted in a yellow-orange coloration. Magnification:  $400\times$ .

of *A. testudineus* express a more efficient mechanism of active ammonia excretion involving Rhag and Rhcg2 in an ammonia-inducible type of Nka-immunoreactive ionocyte, in order to continuously excrete ammonia against inwardly driven  $\text{P}_{\text{NH}_3}$  and  $\text{NH}_4^+$  concentration gradients.

#### Ammonia exposure induces the formation of Nka $\alpha 1\text{c}$ -immunoreactive ionocytes in the gills of *A. testudineus*

Loong et al. (2011) reported that the mRNA and protein expression levels of *nkcc1a/Nkcc1a* increased significantly in the gills of *A. testudineus* exposed to  $100 \text{ mmol l}^{-1} \text{ NH}_4\text{Cl}$  in freshwater, indicating a functional role of Nkcc1a in active ammonia excretion. They proposed that  $\text{NH}_4^+$  entered an ammonia-induced type of ionocyte through the basolateral Nkcc1a before being actively transported across the apical membrane. However, using an antibody raised specifically against Nkcc1a of *A. testudineus*, we obtained results indicating that Nkcc1a was not expressed in the basolateral membranes of the Nka $\alpha 1\text{c}$ -labelled ionocytes in the gills of *A. testudineus* exposed to  $\text{NH}_4\text{Cl}$  (X.L.C. and Y.K.L., unpublished results). By contrast, with the comprehensive anti-NKCC/NCC mouse monoclonal antibody (T4; Developmental

Studies Hybridoma Bank), immunofluorescence was detected along the basolateral membrane of the Nka $\alpha 1\text{c}$ -labelled ionocytes, thereby denoting the presence of a basolateral Nkcc isoform that was different from Nkcc1a. Hence, it is highly probable that active excretion of  $\text{NH}_4^+$  may involve a different isoform of Nkcc1, the identity of which is uncertain at present. In addition, there is a significant increase (12-fold) in the mRNA expression level of *cfr* in the gills of *A. testudineus* exposed to ammonia, and Cfr is expressed in a type of Nka-immunoreactive cell that is different from the type involved in seawater acclimation (Ip et al., 2012b). As CFTR functions as an ATP-powered ‘pump’ (Csanády et al., 2010; Miller, 2010), it is probable that  $\text{Cl}^-/\text{HCO}_3^-$  excretion through Cfr in the gills of *A. testudineus* can generate a favorable electrical potential (inside positive) across the apical membrane to drive the excretion of  $\text{NH}_4^+$  down its electrochemical gradient (but against a concentration gradient) through a yet-to-be-determined transporter (Ip et al., 2012b).

The operation of Nkcc1 during active ammonia excretion would lead to an increase in the intracellular  $\text{Na}^+$  concentration of the ionocytes, and therefore an upregulation of Nka activity would be necessary to remove the excess  $\text{Na}^+$ . The gills of *A. testudineus*



express *nkaα1a*, *nkaα1b* and *nkaα1c*, and ammonia exposure led to significant increases in the mRNA expression of *nkaα1c*, overall Nka protein abundance, Nka activity, and the  $K_m$  for  $K^+$  and  $NH_4^+$  in the gills of *A. testudineus* (Ip et al., 2012a). There was a decrease in the effectiveness of  $NH_4^+$  to substitute for  $K^+$  in the activation of Nka from the gills of fish exposed to ammonia as compared with those of the freshwater control. Hence, the upregulation of *nkaα1c* expression serves to remove excess  $Na^+$  from, and to transport  $K^+$  in preference to  $NH_4^+$  into the cell in order to maintain intracellular  $Na^+$  and  $K^+$  homeostasis (Ip et al., 2012a). Indeed, we demonstrate for the first time through immunofluorescence microscopy that ammonia exposure induced the expression of Nkaα1c-immunoreactive ionocytes, which probably participate in active ammonia excretion, in the gills of *A. testudineus*.

### The Nkaα1c-immunoreactive ionocytes uniquely expressed apical Rhag and basolateral Rhcg2

In fishes, Rhag is generally expressed in red blood cells and erythroid tissues (Hung et al., 2007; Nawata et al., 2007; Tsui et al., 2009). Although Rhag has been detected in the branchial epithelia of several fish species (Nakada et al., 2007a; Claiborne et al., 2008; Braun et al., 2009a,b), it is not known to be associated with the apical membrane of ionocytes. By contrast, the Nkaα1c-immunoreactive ionocyte of *A. testudineus* uniquely expressed Rhag at the apical membrane. Furthermore, Cfr is expressed on the apical membrane of the same ionocyte as apical Rhag in the gills of the ammonia-exposed fish, thereby indicating that Rhag could be the putative  $NH_4^+$  transporter working in conjunction with the apical Cfr in active  $NH_4^+$  excretion. Immunofluorescence microscopy also revealed novel localization of Rhcg2 in the gills of *A. testudineus*; it was localized to the basolateral membranes of Nkaα1a- or Nkaα1c-labelled ionocytes. This is in contrast with the apical localization of Rhcg2 in the pavement cells of the sculpin and

pufferfish (Nakada et al., 2007a; Claiborne et al., 2008). Furthermore, Rhcg2 (in ionocytes) and Rhcg1 (in non-ionocytes) were expressed in different cell types. Hence, during active ammonia excretion,  $NH_4^+$  may enter the ionocytes through either the basolateral Nkcc1 or the basolateral Rhcg2, or both (Fig. 10).

### Do Rhgp, particularly Rhag, transport $NH_3$ or $NH_4^+$ ?

At a physiological pH of ~7.2–7.4,  $NH_4^+$  is the predominant form (95–99%) of ammonia in solution, and it should effectively be the species of ammonia transported by Rhgp. Yet, high-resolution structures of the AMT/Rh/MEP family (Khademi et al., 2004; Zheng et al., 2004; Andrade et al., 2005; Lupo et al., 2007; Li et al., 2007; Gruswitz et al., 2010) show that they exist as homotrimers with highly hydrophobic substrate-conducting pores, suggesting that electroneutral  $NH_3$  is the transporting species. Nonetheless, recent functional studies have provided evidence for the role of Rhgp in  $NH_4^+$  transport (see review by Nakhoul and Hamm, 2014). Expression of pufferfish Rhag, Rhbg, Rhcg1 and Rhcg2 in *Xenopus* oocytes mediates transport of methylammonium (Nakada et al., 2007a). A decrease in intracellular pH and depolarization of the cell has been detected in oocytes expressing RhAG, indicating net  $NH_4^+$  transport (Stewart et al., 2011). Changes in whole cell currents, surface pH and intracellular pH induced by  $NH_3/NH_4^+$  and methyl amine/methyl ammonium have been recorded in *Xenopus* oocytes expressing RhAG, RhBG and RhCG (Caner et al., 2015). These results indicate that RhAG and RhBG transport both  $NH_4^+$  and  $NH_3$  and that the transport of  $NH_4^+$  is electrogenic and not coupled to  $H^+$  efflux. Therefore, it is logical to deduce that Rhag could act as an apical  $NH_4^+$  transporter in the Nkaα1c-immunoreactive ionocytes of *A. testudineus*, facilitating  $NH_4^+$  transport down an electrical potential generated by the active excretion of anion ( $Cl^-/HCO_3^-$ ) through Cfr (Ip et al., 2012b) across the apical membrane (Fig. 10).

### Acknowledgements

We thank Professor S. Hirose for the generous supply of the anti-Rhcg1 antibody.

### Competing interests

The authors declare no competing or financial interests.

### Author contributions

Conceptualization: Y.K.I.; Methodology: Y.K.I.; Formal analysis: X.L.C., B.Z., S.F.C.; Resources: Y.R.C., J.L.O., W.P.W., T.N.; Data curation: X.L.C., B.Z., S.F.C.; Writing - original draft: X.L.C.; Writing - review & editing: X.L.C., Y.K.I.; Supervision: Y.K.I.; Project administration: S.H.L., Y.K.I.; Funding acquisition: S.H.L., Y.K.I.

### Funding

This study was supported by the National Research Foundation Singapore under its Environment & Water Research Programme and administered by the Public Utilities Board - Singapore, Singapore's National Water Agency [grants 2P 10004/82 and 1301-IRIS-23 to S.H.L. and Y.K.I.].

### Supplementary information

Supplementary information available online at <http://jeb.biologists.org/lookup/doi/10.1242/jeb.157123.supplemental>

### References

- Andrade, S. L. A., Dickmanns, A., Ficner, R. and Einsle, O. (2005). Crystal structure of the archaeal ammonium transporter Amt-1 from *Archaeoglobus fulgidus*. *Proc. Natl. Acad. Sci. USA* **102**, 14994–14999.
- Baday, S., Orabi, E. A., Wang, S., Lamoureux, G. and Bernèche, S. (2015). Mechanism of  $NH_4^+$  recruitment and  $NH_3$  transport in Rh proteins. *Structure* **23**, 1550–1557.
- Bakouh, N., Benjelloun, F., Hulin, P., Brouillard, F., Edelman, A., Cherif-Zahar, B. and Planelles, G. (2004).  $NH_3$  is involved in the  $NH_4^+$  transport induced by the functional expression of the human Rh C glycoprotein. *J. Biol. Chem.* **279**, 15975–15983.
- Benjelloun, F., Bakouh, N., Fritsch, J., Hulin, P., Lipecka, J., Edelman, A., Planelles, G., Thomas, S. R. and Cherif-Zahar, B. (2005). Expression of the

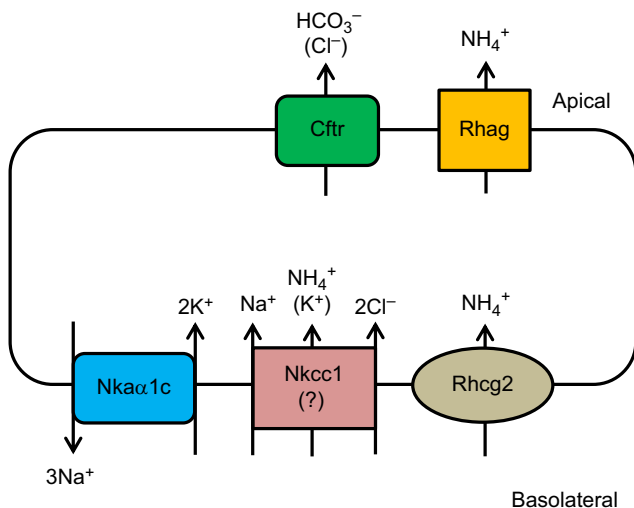


**Fig. 10. Proposed model of an ammonia-type ionocyte (Nkaα1c-labelled) in the gills of *Anabas testudineus* involved in active  $NH_4^+$  excretion.**  $NH_4^+$  could enter the basolateral membrane through Rhcg2 or an Nkcc1 isoform (the identity of which is uncertain at present), and exit the ionocytes via apical Rhag. The transport of  $NH_4^+$  is driven by an electrical potential generated by the active excretion of anion through Cfr. Cfr, cystic fibrosis transmembrane conductance regulator  $Cl^-$  channel; Nkaα1c,  $Na^+/K^+$ -ATPase α1c; Nkcc1,  $Na^+:K^+:2Cl^-$  cotransporter 1; Rhag, rhesus blood group-associated glycoprotein; Rhcg2, rhesus family C glycoprotein 2. Based on results from Figs. 6 and 9.

- human erythroid Rh glycoprotein (RhAG) enhances both  $\text{NH}_3$  and  $\text{NH}_4^+$  transport in HeLa cells. *Pflügers Arch.* **450**, 155–167.
- Bergmeyer, H. U. and Beutler, H. O.** (1985). Ammonia. In *Methods of Enzymatic Analysis*, Vol VIII (ed. H. U. Bergmeyer, J. Bergmeyer and M. Grassl), pp. 454–461. New York: Academic Press.
- Bradford, M. M.** (1976). A rapid and sensitive method for the quantitation of microgram quantities of protein utilizing the principle of protein–dye binding. *Anal. Biochem.* **72**, 248–254.
- Braun, M. H., Steele, S. L., Ekker, M. and Perry, S. F.** (2009a). Nitrogen excretion in developing zebrafish (*Danio rerio*): a role for Rh proteins and urea transporters. *Am. J. Physiol. Renal. Physiol.* **296**, F994–F1005.
- Braun, M. H., Steele, S. L. and Perry, S. F.** (2009b). The responses of zebrafish (*Danio rerio*) to high external ammonia and urea transporter inhibition: nitrogen excretion and expression of rhesus glycoproteins and urea transporter proteins. *J. Exp. Biol.* **212**, 3846–3856.
- Caner, T., Abdounour-Nakhoul, S., Brown, K., Islam, M. T., Hamm, L. L. and Nakhoul, N. L.** (2015). Mechanisms of ammonia and ammonium transport by Rhesus-associated glycoproteins. *Am. J. Physiol. Cell Physiol.* **309**, C747–C758.
- Chew, S. F. and Ip, Y. K.** (2014). Excretory nitrogen metabolism and defence against ammonia toxicity in air-breathing fishes. *J. Fish Biol.* **84**, 603–638.
- Ching, B., Chen, X. L., Yong, J. H. A., Wilson, J. M., Hiong, K. C., Sim, W. L. E., Wong, W. P., Lam, S. H., Chew, S. F. and Ip, Y. K.** (2013). Increases in apoptosis, caspase activity and expression of *p53* and *bax*, and the transition between two types of mitochondrion-rich cells, in the gills of the climbing perch, *Anabas testudineus*, during a progressive acclimation from freshwater to seawater. *Front. Physiol.* **4**, 1–21.
- Claiborne, J. B., Kratochvilova, H., Diamanduros, A. W., Hall, C., Phillips, M. E., Hirose, S. and Edwards, S.** (2008). Expression of branchial Rh glycoprotein ammonia transporters in the marine longhorn sculpin (*Myoxocephalus octodecemspinosus*). *Bull. Mt. Desert Is. Biol. Lab. Salisb. Cove Maine* **47**, 67–68.
- Csanády, L., Vergani, P. and Gadsby, D. C.** (2010). Strict coupling between CFTR's catalytic cycle and gating of its  $\text{Cl}^-$  ion pore revealed by distributions of open channel burst durations. *Proc. Natl. Acad. Sci. USA* **107**, 1241–1246.
- Evans, D. H., Piermarini, P. M. and Choe, K. P.** (2005). The multifunctional fish gill: dominant site of gas exchange, osmoregulation, acid-base regulation, and excretion of nitrogenous waste. *Physiol. Rev.* **85**, 97–177.
- Fong, R. N., Kim, K.-S., Yoshihara, C., Inwood, W. B. and Kustu, S.** (2007). The W148L substitution in the *Escherichia coli* ammonium channel AmtB increases flux and indicates that the substrate is an ion. *Proc. Natl. Acad. Sci. USA* **104**, 18706–18711.
- Gerwick, L., Corley-Smith, G. and Bayne, C. J.** (2007). Gene transcript changes in individual rainbow trout livers following an inflammatory stimulus. *Fish Shellfish Immunol.* **22**, 157–171.
- Graham, J. B.** (1997). *Air-Breathing Fishes*. San Diego, CA: Academic Press.
- Gruswitz, F., Chaudhary, S., Ho, J. D., Schlessinger, A., Pezeshki, B., Ho, C.-M., Sali, A., Westhoff, C. M. and Stroud, R. M.** (2010). Function of human Rh based on structure of RhCG at 2.1 Å. *Proc. Natl. Acad. Sci. USA* **107**, 9638–9643.
- Hall, T. A.** (1999). BioEdit: a user-friendly biological sequence editor and analysis program for Windows 95/98/NT. *Nucl. Acids Symp. Ser.* **41**, 95–98.
- Hall, J. A. and Kustu, S.** (2011). The pivotal twin histidines and aromatic triad of the *Escherichia coli* ammonium channel AmtB can be replaced. *Proc. Natl. Acad. Sci. USA* **108**, 13270–13274.
- Huang, C.-H. and Peng, J.** (2005). Evolutionary conservation and diversification of Rh family genes and proteins. *Proc. Natl. Acad. Sci. USA* **102**, 15512–15517.
- Hughes, G. M. and Munshi, J. S. D.** (1973). Fine structure of the respiratory organs of the climbing perch, *Anabas testudineus* (Pisces: Anabantidae). *J. Zool.* **170**, 201–225.
- Hung, C. Y. C., Tsui, K. N. T., Wilson, J. M., Nawata, C. M., Wood, C. M. and Wright, P. A.** (2007). Rhesus glycoprotein gene expression in the mangrove killifish *Kryptolebias marmoratus* exposed to elevated environmental ammonia levels and air. *J. Exp. Biol.* **210**, 2419–2429.
- Hwang, P.-P., Lee, T.-H. and Lin, L.-Y.** (2011). Ion regulation in fish gills: recent progress in the cellular and molecular mechanisms. *Am. J. Physiol. Regul. Integr. Comp. Physiol.* **301**, R28–R47.
- Ip, Y. K. and Chew, S. F.** (2010). Ammonia production, excretion, toxicity and defense in fish: a review. *Front. Physiol.* **1**, 1–20.
- Ip, Y. K., Loong, A. M., Kuah, J. S., Sim, E. W. L., Chen, X. L., Wong, W. P., Lam, S. H., Delgado, I. L. S., Wilson, J. M. and Chew, S. F.** (2012a). The roles of three branchial  $\text{Na}^+/\text{K}^+$ -ATPase  $\alpha$ -subunit isoforms in freshwater adaptation, seawater acclimation and active ammonia excretion in *Anabas testudineus*. *Am. J. Physiol. Regul. Integr. Comp. Physiol.* **303**, R112–R125.
- Ip, Y. K., Wilson, J. M., Loong, A. M., Chen, X. L., Wong, W. P., Delgado, I. L. S., Lam, S. H. and Chew, S. F.** (2012b). Cystic fibrosis transmembrane conductance regulator in the gills of the climbing perch, *Anabas testudineus*, is involved in both hypoosmotic regulation during seawater acclimation and active ammonia excretion during ammonia exposure. *J. Comp. Physiol. B* **182**, 793–812.
- Khademi, S. and Stroud, R. M.** (2006). The Amt/MEP/Rh Family: structure of AmtB and the mechanism of ammonia gas conduction. *Physiology* **21**, 419–429.
- Khademi, S., O'Connell, J., III, Remis, J., Robles-Colmenares, Y., Miercke, L. J. and Stroud, R. M.** (2004). Mechanism of ammonia transport by Amt/MEP/Rh: structure of AmtB at 1.35 Å. *Science* **305**, 1587–1594.
- Laemmli, U. K.** (1970). Cleavage of structural proteins during the assembly of the head of bacteriophage T4. *Nature* **227**, 680–685.
- Li, X., Jayachandran, S., Nguyen, H.-H. T. and Chan, M. K.** (2007). Structure of the *Nitrosomonas europaea* Rh protein. *Proc. Natl. Acad. Sci. USA* **104**, 19279–19284.
- Loong, A. M., Chew, S. F., Wong, W. P., Lam, S. H. and Ip, Y. K.** (2011). Both seawater acclimation and environmental ammonia exposure lead to increases in mRNA expression and protein abundance of  $\text{Na}^+/\text{K}^+:\text{2Cl}^-$  cotransporter in the gills of the climbing perch, *Anabas testudineus*. *J. Comp. Physiol. B* **182**, 491–506.
- Loqué, D., Mora, S. I., Andrade, S. L. A., Pantoja, O. and Frommer, W. B.** (2009). Pore mutations in ammonium transporter AMT1 with increased electrogenic ammonium transport activity. *J. Biol. Chem.* **284**, 24988–24995.
- Lupo, D., Li, X.-D., Durand, A., Tomizaki, T., Cherif-Zahar, B., Matassi, G., Merrick, M. and Winkler, F. K.** (2007). The 1.3-Å resolution structure of *Nitrosomonas europaea* Rh50 and mechanistic implications for  $\text{NH}_3$  transport by Rhesus family proteins. *Proc. Natl. Acad. Sci. USA* **104**, 19303–19308.
- Marini, A. M., Vissers, S., Urrestarazu, A. and Andre, B.** (1994). Cloning and expression of the MEP1 gene encoding an ammonium transporter in *Saccharomyces cerevisiae*. *EMBO J.* **13**, 3456–3463.
- Marini, A. M., Matassi, G., Raynal, V., André, B., Cartron, J.-P. and Chérif-Zahar, B.** (2000). The human Rhesus-associated RhAG protein and a kidney homologue promote ammonium transport in yeast. *Nat. Genet.* **26**, 341–344.
- McGuffin, L. J., Bryson, K. and Jones, D. T.** (2000). The PSIPRED protein structure prediction server. *Bioinformatics* **16**, 404–405.
- Miller, C.** (2010). CFTR: break a pump, make a channel. *Proc. Natl. Acad. Sci. USA* **107**, 959–960.
- Moreira-Silva, J., Tsui, T. K. N., Coimbra, J., Vijayan, M. M., Ip, Y. K. and Wilson, J. M.** (2010). Branchial ammonia excretion in the Asian weatherloach *Misgurnus anguillicaudatus*. *Comp. Biochem. Physiol. C Toxicol. Pharmacol.* **151**, 40–50.
- Munshi, J. S. D., Olson, K. R., Ojha, J. and Ghosh, T. K.** (1986). Morphology and vascular anatomy of the accessory respiratory organs of the air-breathing climbing perch, *Anabas testudineus* (Bloch). *Am. J. Anat.* **176**, 321–331.
- Nakada, T., Westhoff, C. M., Kato, A. and Hirose, S.** (2007a). Ammonia secretion from fish gill depends on a set of Rh glycoproteins. *FASEB J.* **21**, 1067–1074.
- Nakada, T., Hoshijima, K., Esaki, M., Nagayoshi, S., Kawakami, K. and Hirose, S.** (2007b). Localization of ammonia transporter Rhcg1 in mitochondrion-rich cells of yolk sac, gill, and kidney of zebrafish and its ionic strength-dependent expression. *Am. J. Physiol. Regul. Integr. Comp. Physiol.* **293**, R1743–R1753.
- Nakhoul, N. L. and Hamm, L. L.** (2013). Characteristics of mammalian Rh glycoproteins (SLC42 transporters) and their role in acid–base transport. *Mol. Aspects Med.* **34**, 629–637.
- Nakhoul, N. L. and Hamm, L. L.** (2014). The challenge of determining the role of Rh glycoproteins in transport of  $\text{NH}_3$  and  $\text{NH}_4^+$ . *Wiley. Interdiscip. Rev. Membr. Transp. Signal* **3**, 53–61.
- Nakhoul, N. L., Schmidt, E., Abdounour-Nakhoul, S.-M. and Hamm, L. L.** (2006). Electrogenic ammonium transport by renal Rhbg. *Transfus. Clin. Biol.* **13**, 147–153.
- Namimatsu, S., Ghazizadeh, M. and Sugisaki, Y.** (2005). Reversing the effects of formalin fixation with citraconic anhydride and heat: a universal antigen retrieval method. *J. Histochem. Cytochem.* **53**, 3–11.
- Nawata, C. M. and Wood, C. M.** (2009). mRNA expression analysis of the physiological responses to ammonia infusion in rainbow trout. *J. Comp. Physiol. B* **179**, 799–810.
- Nawata, C. M., Hung, C. C. Y., Tsui, T. K. N., Wilson, J. M., Wright, P. A. and Wood, C. M.** (2007). Ammonia excretion in rainbow trout (*Oncorhynchus mykiss*): evidence for Rh glycoprotein and  $\text{H}^+$ -ATPase involvement. *Physiol. Genomics* **31**, 463–474.
- Nawata, C. M., Hirose, S., Nakada, T., Wood, C. M. and Kato, A.** (2010). Rh glycoprotein expression is modulated in pufferfish (*Takifugu rubripes*) during high environmental ammonia exposure. *J. Exp. Biol.* **213**, 3150–3160.
- Ninnemann, O., Jauniaux, J. C. and Frommer, W. B.** (1994). Identification of a high affinity  $\text{NH}_4^+$  transporter from plants. *EMBO J.* **13**, 3464–3471.
- Pethiyagoda, R.** (1991). *Freshwater Fishes of Sri Lanka*. p. 362. Colombo: The Wildlife Heritage Trust of Sri Lanka.
- Ripoche, P., Bertrand, O., Gane, P., Birkenmeier, C., Colin, Y. and Cartron, J.-P.** (2004). Human Rhesus-associated glycoprotein mediates facilitated transport of  $\text{NH}_3$  into red blood cells. *Proc. Natl. Acad. Sci. USA* **101**, 17222–17227.
- Stewart, A. K., Shmukler, B. E., Vandorpe, D. H., Rivera, A., Heneghan, J. F., Li, X., Hsu, A., Karpattin, M., O'Neill, A. F., Bauer, D. E. et al.** (2011). Loss-of-function and gain-of-function phenotypes of stomatocytosis mutant RhAG F65S. *Am. J. Physiol. Cell Physiol.* **301**, C1325–C1343.
- Tay, Y. L., Loong, A. M., Hiong, K. C., Lee, S. J., Tng, Y. Y. M., Wee, N. L. J., Lee, S. M. L., Wong, W. P., Chew, S. F., Wilson, J. M. et al.** (2006). Active ammonia transport and excretory nitrogen metabolism in the climbing perch, *Anabas testudineus*, during 4 days of emersion or 10 minutes of forced exercise on land. *J. Exp. Biol.* **209**, 4475–4489.

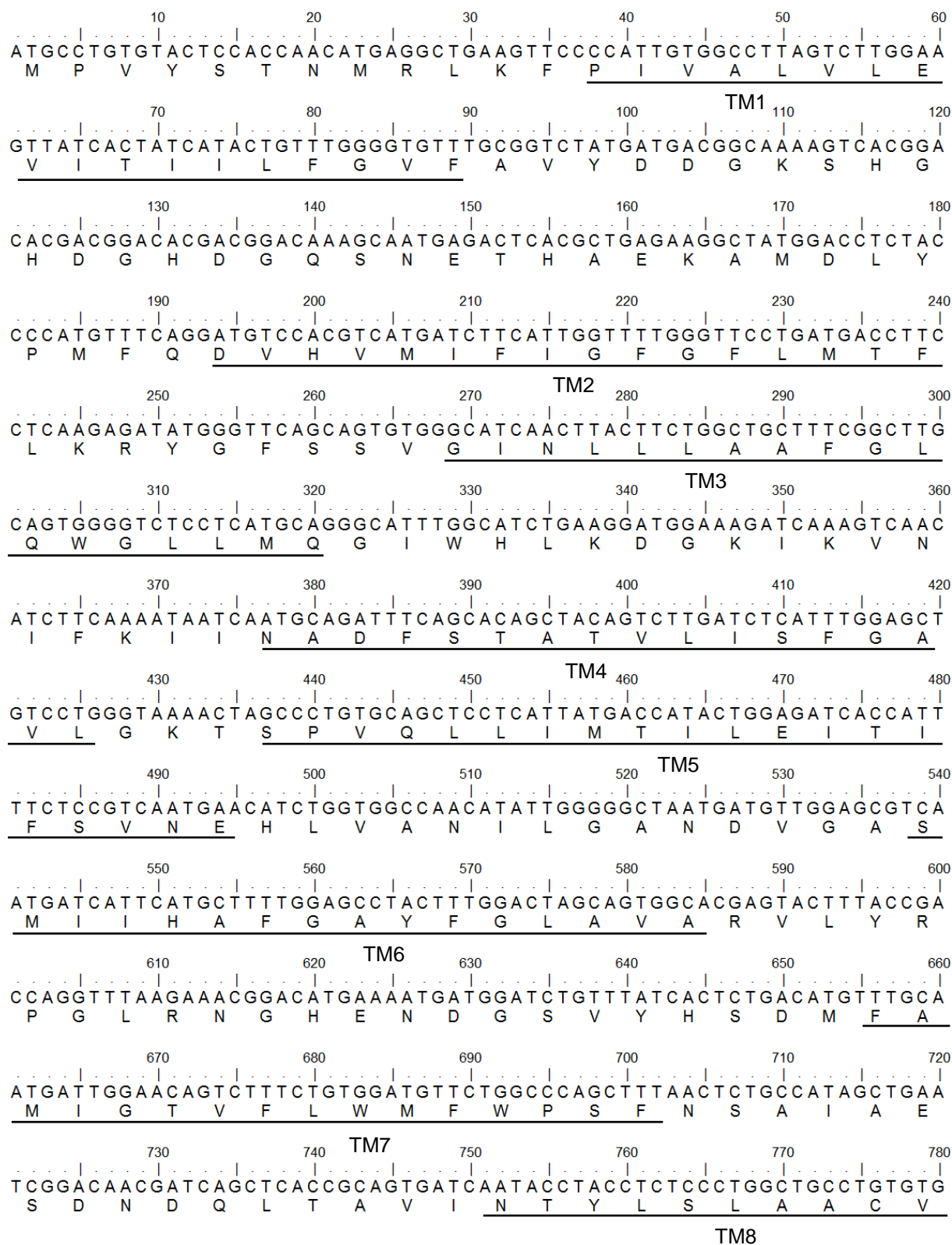
- Tsui, T. K. N., Hung, C. Y. C., Nawata, C. M., Wilson, J. M., Wright, P. A., Wood, C. M.** (2009). Ammonia transport in cultured gill epithelium of freshwater rainbow trout: the importance of Rhesus glycoproteins and the presence of an apical  $\text{Na}^+/\text{NH}_4^+$  exchange complex. *J. Exp. Biol.* **212**, 878-892.
- Ura, K., Soyano, K., Omoto, N., Adachi, S. and Yamauchi, K.** (1996). Localization of  $\text{Na}^+, \text{K}^+$ -ATPase in tissues of rabbit and teleosts using an antiserum directed against a partial sequence of the  $\alpha$ -subunit. *Zool. Sci.* **13**, 219-227.
- Wang, J., Fulford, T., Shao, Q., Javelle, A., Yang, H., Zhu, W. and Merrick, M.** (2013). Ammonium transport proteins with changes in one of the conserved pore histidines have different performance in ammonia and methylamine conduction. *PLoS ONE* **8**, e62745.
- Weihrauch, D., Wilkie, M. P. and Walsh, P. J.** (2009). Ammonia and urea transporters in gills of fish and aquatic crustaceans. *J. Exp. Biol.* **212**, 1716-1730.
- Wilkie, M. P.** (1997). Mechanisms of ammonia excretion across fish gills. *Comp. Biochem. Physiol. A* **118**, 39-50.
- Wilkie, M. P.** (2002). Ammonia excretion and urea handling by fish gills: present understanding and future research challenges. *J. Exp. Zool.* **293**, 284-301.
- Wood, C. M. and Nawata, C. M.** (2011). A nose-to-nose comparison of the physiological and molecular responses of rainbow trout to high environmental ammonia in seawater versus freshwater. *J. Exp. Biol.* **214**, 3557-3569.
- Wright, P. A. and Wood, C. M.** (2009). A new paradigm for ammonia excretion in aquatic animals: role of Rhesus (Rh) glycoproteins. *J. Exp. Biol.* **212**, 2303-2312.
- Wu, S.-C., Horng, J.-L., Liu, S.-T., Hwang, P.-P., Wen, Z.-H., Lin, C.-S. and Lin, L.-Y.** (2010). Ammonium-dependent sodium uptake in mitochondrion-rich cells of medaka (*Oryzias latipes*) larvae. *Am. J. Physiol. Cell Physiol.* **298**, C237-C250.
- Zheng, L., Kostrewa, D., Berneche, S., Winkler, F. K. and Li, X.-D.** (2004). The mechanism of ammonia transport based on the crystal structure of AmtB of *Escherichia coli*. *Proc. Natl. Acad. Sci. USA* **101**, 17090-17095.
- Zidi-Yahiaoui, N., Ripoché, P., Le Van Kim, C., Gane, P., D'Ambrosio, A.-M., Cartron, J.-P., Colin, Y. and Mouro-Chanteloup, I.** (2006). Ammonium transport properties of HEK293 cells expressing RhCG mutants: preliminary analysis of structure/function by site-directed mutagenesis. *Transfus. Clin. Biol.* **13**, 128-131.



**Table S1.** Primers used for RACE-PCR and quantitative real-time PCR on *rhesus blood group-associated glycoprotein (rhag)*, *rhesus family B glycoprotein (rhbg)*, *rhesus family C glycoprotein 1 (rhcg1)* and *rhesus family C glycoprotein 2 (rhcg2)* from the gills of *Anabas testudineus*.

Gene	Primer type		Primer sequence
<i>rhag</i>	RACE-PCR	5'-RACE	5'-CAGCCACAATACCAGCCAAACCTCC-3'
		3'-RACE	5'-GGAGCACAAAGGGAAACTGGACA-3'
	qPCR	Forward	5'-CGCTGACATGAGCATCGG-3'
		Reverse	5'-CTACAGCCACAATACCAGCC-3'
<i>rhbg</i>	RACE-PCR	5'-RACE	5'-GGATGGGTGTGAGATACTTGAAGCC-3'
		3'-RACE	5'-ACACCTACTACTCCCTGGCTG-3'
	qPCR	Forward	5'-GCTCACCTGCTTCATCCT-3'
		Reverse	5'-TGCCATTTCTTTGCATCCGT-3'
<i>rhcg1</i>	RACE-PCR	5'-RACE	5'-CCTCCCAGTAGACCTCATCATTAAAGC-3'
		3'-RACE	5'-GCTGCATCTGTTCTCACCCTG-3'
	qPCR	Forward	5'-TATCCTGAACCTCATAACGCT-3'
		Reverse	5'-CCTGTAGACGACTGCTCTG-3'
<i>rhcg2</i>	RACE-PCR	5'-RACE	5'-CCTTCCAAGCCAAGTGTAGCAATCA-3'
		3'-RACE	5'-CAGCCATAAACACTTACATCTC-3'
	qPCR	Forward	5'-TGGGAGATTGCTATGGTTGTG-3'
		Reverse	5'-ATGTCGGTGGTGATGTTGTG-3'

**Fig. S1.** The nucleotide sequence and the translated amino acid sequence of the coding region of *rhesus-associated glycoprotein (rhag*; Genbank accession number KF830708) from the gills of *Anabas testudineus*. The 12 predicted transmembrane regions are underlined.



790 800 810 820 830 840  
CTCTCTGCCTACGCCATATCCAGCCTTGTGGAGCACAAAGGGAAACTGGACATGGTGCAC  
L S A Y A I S S L V E H K G K L D M V H

850 860 870 880 890 900  
ATCCAGAATGCCACCTTGGCTGGCGGTGTGGCCGTGGGAACATGCGCTGACATGAGCATC  
I Q N A T L A G G V A V G T C A D M S I

910 920 930 940 950 960  
GGACCAGTGGGAGCCATGGTGTATTGGATTTGTGGCCGGCATCATCTCTACCTTGGGTTT  
G P V G A M V I G F V A G I I S T L G F

970 980 990 1000 1010 1020  
AAGTACCTATCGCCCATCCTGGCATCCAAGCTGGGCATCCAGGATACCTGTGGTGTCCAC  
K Y L S P I L A S K L G I Q D T C G V H

1030 1040 1050 1060 1070 1080  
AATCTGCATGGCATGCCTGGCATCCTGGGAGGTTTGGCTGGTATTGTGGCTGTAGCCTTG  
N L H G M P G I L G G L A G I V A V A L

1090 1100 1110 1120 1130 1140  
GGAAAGAAAAAGGTGAAGCTACCATGCAAGCTGCTGCCTTGGGTTTCATCCCTTGGGTTT  
G K K K G E A T M Q A A A L G S S L G F

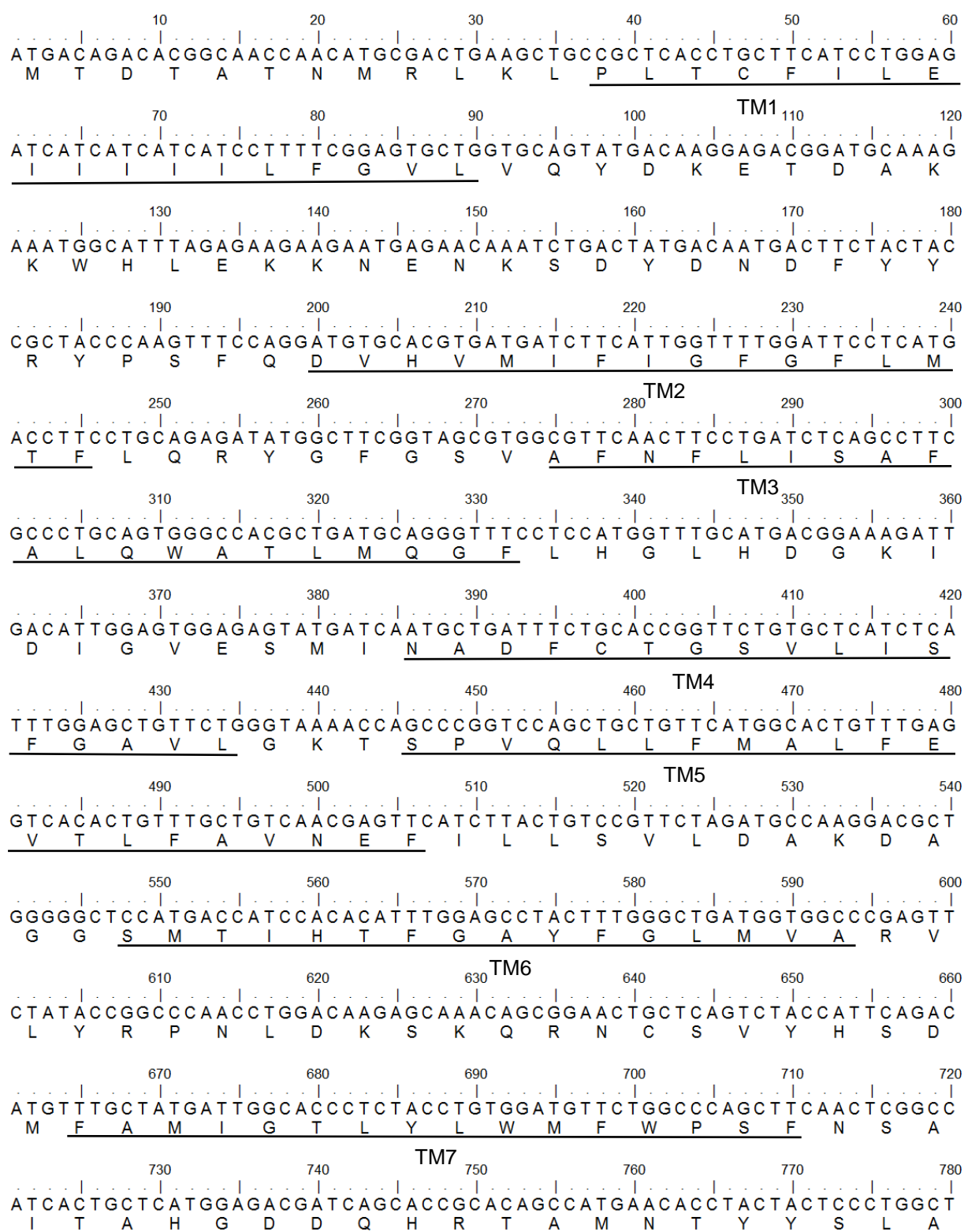
1150 1160 1170 1180 1190 1200  
GCGTTGGTTGGAGGTGCTCTTACAGGTTTAATAATGAAGTTGCCAATCTGGGGACAGCCT  
A L V G G A L T G L I M K L P I W G Q P

1210 1220 1230 1240 1250 1260  
CCAGACCAGAACTGCTTTGATGACTCTGTTTACTGGGAGGTTCCCGAGGAAGAGGAGGAA  
P D Q N C F D D S V Y W E V P E E E E E

1270 1280 1290 1300 1310  
AATGAGGAGAGCTTGGCACACGCTGATCACTCAAAGAATAAAACAGAGGCT  
N E E S L A H A D H S K N K T E A



**Fig. S2.** The nucleotide sequence and the translated amino acid sequence of the coding region of *rhesus family B glycoprotein (rhbg; KF830709)* in the gills of *Anabas testudineus*. The 11 predicted transmembrane regions are underlined.



790 800 810 820 830 840  
GCCTGCACTCTGTCCACCTTCGCTATGTCTCACTCACGGCACATGACGGCAAGCTGGAC  
A C T L S T F A M S S L T A H D G K L D

850 860 870 880 890 900  
ATGGTCCACATTCAAATGCAGCTCTGGCAGGTGGAGTCGCAGCGGGAACGGCTGGTGAA  
M V H I Q N A A L A G G V A A G T A G E

910 920 930 940 950 960  
ATGATGCTGACACCTGTTGGCTCTATGATTGTTGGTTTCTTGGCCGGCATCATCTCTGTG  
M M L T P V G S M I V G F L A G I I S V

970 980 990 1000 1010 1020  
CTGGGCTTCAAGTATCTCACACCCATCCTGGAGGAGAAACTGAAGATCCAAGATACCTGC  
L G F K Y L T P I L E E K L K I Q D T C

1030 1040 1050 1060 1070 1080  
GGGTTTCAACAACCTGCACGGCATGCCCGGCGTCTGGGTGCTATTGTGGGAGCGGTGACA  
G V H N L H G M P G V L G A I V G A V T

1090 1100 1110 1120 1130 1140  
GCTTCTCTGGCATCCAGAGAAGTTTATGGAGATGGTTTGGAAAGACGTCTTCCCAAATA  
A S L A S R E V Y G D G L E D V F P K I

1150 1160 1170 1180 1190 1200  
GCAAAATGGAGATTTAAGTGCCTCGACCCAGGGATTTTCGTCAGGCCATCTCCCTTGGTGTC  
A N G D L S A S T Q G F R Q A I S L G V

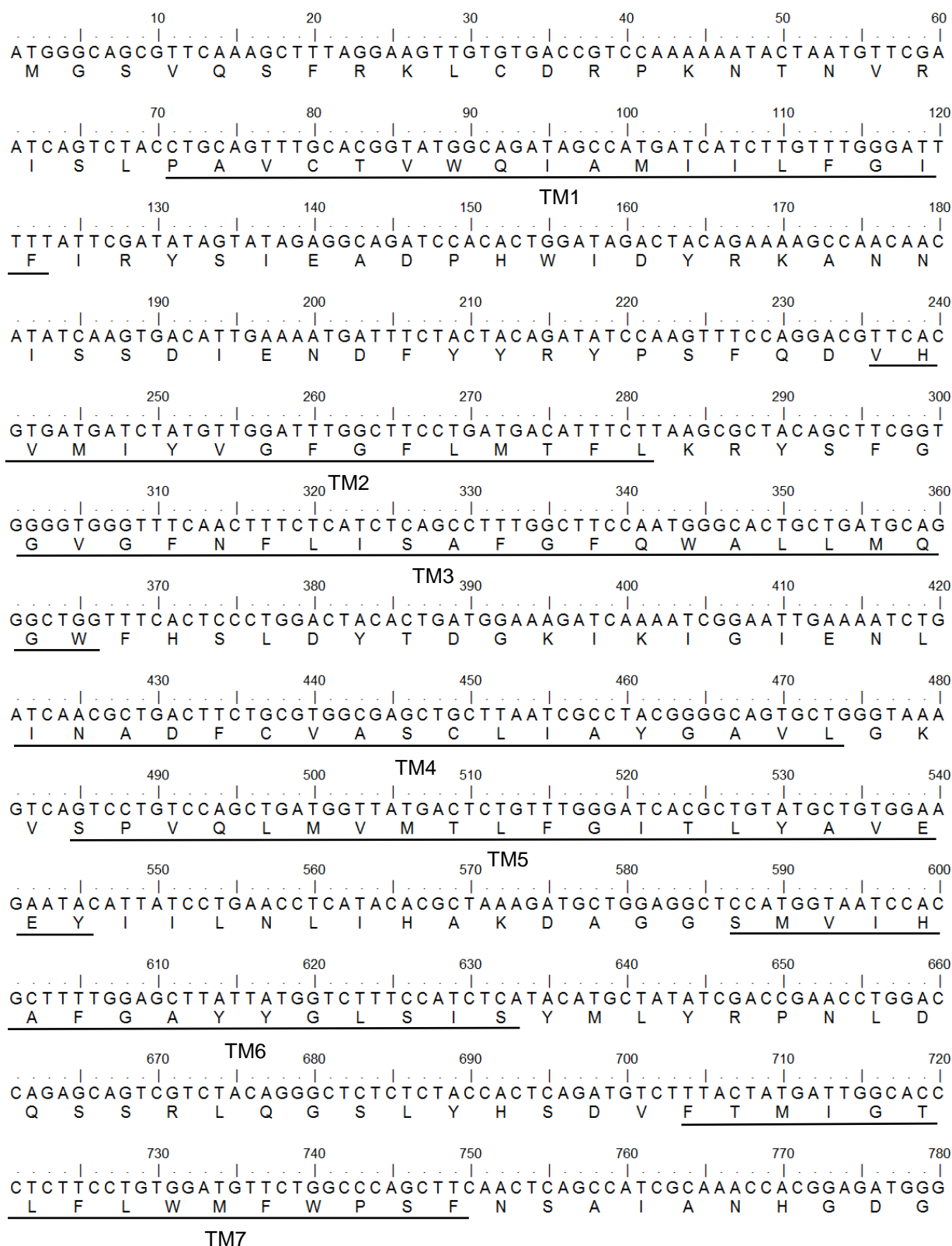
1210 1220 1230 1240 1250 1260  
ACTCTGGGTATAGCCCTGCTGGGAGGGATTGTTGTCTGGTTTTATTTTGAAGCTGCCAGTC  
T L G I A L L G G I V V G F I L K L P V

1270 1280 1290 1300 1310 1320  
TGCGGGGCTCCTTCTGACGCCATCTGCTTTGAGGACAACATCTACTGGGAGGTGCCTGAA  
C G A P S D A I C F E D N I Y W E V P E

1330 1340 1350 1360 1370 1380  
GACAGCCCGAGTCACGGGGACCAGCTGGCTAGTGTGAGGACAGAGGAGTCCGAGAAGCTC  
D S P S H G D Q L A S V R T E E S E K L

..|.  
AACAGT  
N S

**Fig. S3.** The nucleotide sequence and the translated amino acid sequence of the coding region of *rhesus family C glycoprotein 1 (rhcg1; KF830710)* in the gills of *Anabas testudineus*. The 11 predicted transmembrane (TM) regions are underlined.





790 800 810 820 830 840  
CAACTCAGAGCAGTCATCAACACCTACCTGTCTTTGGCTGCATCTGTTCTCACCCTGTG  
Q L R A V I N T Y L S L A A S V L T T V

850 860 870 880 890 900  
GTCATATCAAGCCTCTGCAACAAGCACGGGAAACTAGACATGGTTCACATCCAGAACGCC  
V I S S L C N K H G K L D M V H I Q N A

910 920 930 940 950 960  
ACTCTTGCAGGGGGTGTTCAGTGGGAACAGCAGCCGAGTTCATGCTGATGCCCTACGGA  
T L A G G V A V G T A A E F M L M P Y G

970 980 990 1000 1010 1020  
TCTCTGATTGTAGGATTCTGCTGTGGTGTGATCTCCACACTGGGATATGTCTACGTCACG  
S L I V G F C C G V I S T L G Y V Y V T

1030 1040 1050 1060 1070 1080  
CCATTTTTGAAAAACACCTCAAGATCCATGACACATGCGGAGTCCACAACCTTCATGGC  
P F L E K H L K I H D T C G V H N L H G

1090 1100 1110 1120 1130 1140  
ATGCCGCAATCGTAGGAGGCATCGTGGGAGCTGTTACCGCTGCATGTGCAACAGAATCA  
M P A I V G G I V G A V T A A C A T E S

1150 1160 1170 1180 1190 1200  
GCTTATGGCACTGAAGGGCTGATTAGCACCTTCGACTTTACCGGGGACTTCAAAAACATG  
A Y G T E G L I S T F D F T G D F K N M

1210 1220 1230 1240 1250 1260  
ACACCCGCAAAGCAGGGCGGTCACCAGGCTGCAGGCCTCTGTGTGGCTCTCTGTTTTGGA  
T P A K Q G G H Q A A G L C V A L C F G

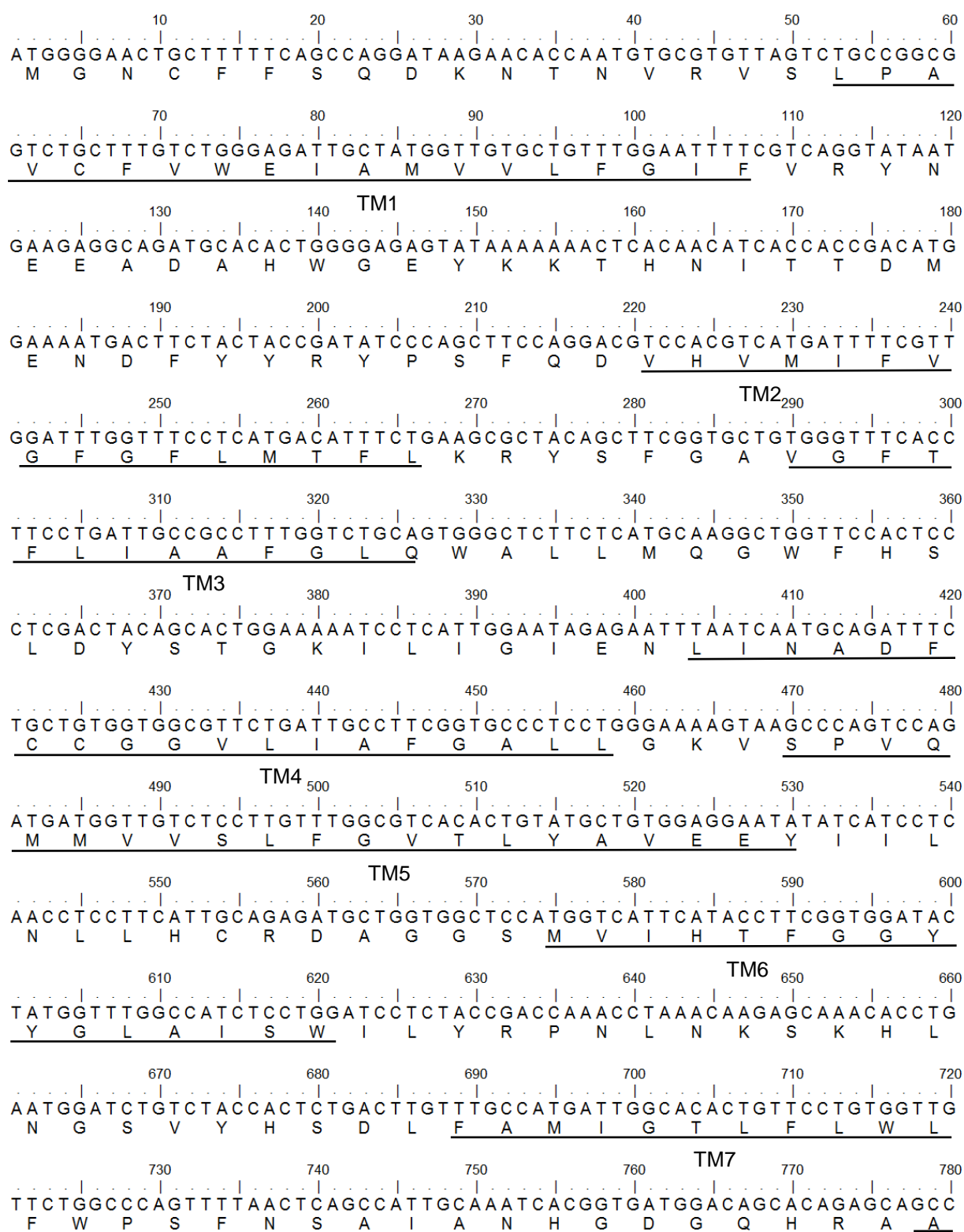
1270 1280 1290 1300 1310 1320  
ATAGGCGGTGGCATCCTTGTTCGGCGCCATCTTAAGATTACCTATATGGGGAGATCCTGCA  
I G G G I L V G A I L R L P I W G D P A

1330 1340 1350 1360 1370 1380  
GATGACAACTGCTTTAATGATGAGGTCTACTGGGAGGTTTCTGAAGATGAAGAGAGCATC  
D D N C F N D E V Y W E V P E D E E S I

1390 1400 1410 1420 1430 1440  
CCTCCCATGATACAGTACAACAACCACATGCAGAGAAAGGATGCATTACCGTCAAATTC  
P P M I Q Y N N H M Q R K D A L P S N F

1450 1460  
ACCTTGGAGCATCAAGATCAC  
T L E H Q D H

**Fig. S4.** The nucleotide sequence and the translated amino acid sequence of the coding region of *rhesus family C glycoprotein 2 (rhcg2; KF830711)* in the gills of *Anabas testudineus*. The 12 predicted transmembrane (TM) regions are underlined.



790 800 810 820 830 840  
A T A A A C A C T T A C A T C T C C C T G G C T G C C T C C G T T G T C A C A G C T G T G G C C A T C T C C A G T A T G  
I N T Y I S L A A S V V T A V A I S S M

850 860 870 880 890 900  
A C T G A G A A G A G A G G A A A A C T G G A T A T G G T G C A T A T C C A G A A T G C C A C T T T G G C A G G T G G T  
T E K R G K L D M V H I Q N A T L A G G

910 920 930 940 950 960  
G T G G C C A T G G G A G C A T C A G C A G A G T T C A T G A T A A G T C C A T A C G G C T C A C T C A T T G T G G G T  
V A M G A S A E F M I S P Y G S L I V G

970 980 990 1000 1010 1020  
T T C T T C T G T G G C A T C A T C T C C A C C T T T G G C T T T A A A T T T G T C T C G C C C T T C T T A G A A A A A  
F F C G I I S T F G F K F V S P F L E K

1030 1040 1050 1060 1070 1080  
C A T C T C A A G C T C C A G G A T A C A T G T G G T A T C C A C A A C C T G C A T G C T G T G C C G G G G A T G C T T  
H L K L Q D T C G I H N L H A V P G M L

1090 1100 1110 1120 1130 1140  
G G C G G A T T T A T C A G T G C C A T C G T T G C A G C A A T G G C C T C T G A A T C T G T C T A C A G C A A A G A G  
G G F I S A I V A A M A S E S V Y S K E

1150 1160 1170 1180 1190 1200  
G G T T G A T T G C T A C A C T T G G C T T G G A A G G C A A T T A T G C A A A C A G A G G T G C A G G T A C G C A G  
G L I A T L G L E G N Y A N R G A G T Q

1210 1220 1230 1240 1250 1260  
G G A G G C T A C C A G G C T G C T G G C A C A T G T G T G G C A A T G G T A T T T G G A A T T G T T G G A G G G G C A  
G G Y Q A A G T C V A M V F G I V G G A

1270 1280 1290 1300 1310 1320  
A T T G T T G G G C T C A T C C T G A A G T T G C C T A T C T G G G G C G A C C C T G C T G A T G A T A A C T G C T T T  
I V G L I L K L P I W G D P A D D N C F

1330 1340 1350 1360 1370 1380  
G A T G A T G A A G T T T A C T G G G A G G T T C C T G A G G A T G A G G A G A G C A T T C C T C C T G T T T T G G A G  
D D E V Y W E V P E D E E S I P P V L E

1390 1400 1410 1420 1430 1440  
T A C A A C A A C C A C A T G G C A C A C A A G C A C C A A G A C A G A T G T G A T T C A A A C T A T A A T C T G G A G  
Y N N H M A H K H Q D R C D S N Y N L E

CAACTT  
Q L



**Fig. S5.** Immunoblot of **(A)** Rhesus blood group-associated glycoprotein (Rhag), **(B)** Rhesus family B glycoprotein (Rhbg), **(C)** Rhesus family C glycoprotein 1 (Rhcg1) or **(D)** Rhesus family C glycoprotein 2 (Rhcg2) pre-incubated with its respective immunizing peptide for the peptide competition assay (PCA). Due to interaction of anti-Rhcg1 with the ladder, the lane containing the ladder was cut out prior to primary antibody incubation and pieced together with the rest of the membrane before scanning. Both the ladder and protein samples were electrophoresed concurrently on the same gel. Site of splicing is denoted by a black line.

